JAERI-M
86-017

CURRENT GENERATION BY A LARGE AMPLITUDE WAVE PACKET

February 1986

Shoji TANAKA*

日本原子力研究所
Japan Atomic Energy Research Institute

JAERI Mレポートは，日本原子力研究所が不定期に公刊している研究報告書です。
入手の問合わせは，日本原子力研究所技術情報部情報資料課（〒319-11 茨城県那珂郡東海村）あて，お申しこしください。なお，このほかに財団法人原子力弘済会資料センター（〒319-11 茨城県那珂郡東海村日本原子力研究所内）で複写による実費領布をおこなっております。

JAERI-M reports are issued irregularly.
Inquiries about availability of the reports should be addressed to Information Division Department of Technical Information, Japan Atomic Energy Research Institute, Tokaimura, Naka-gun, Ibaraki-ken 319-11, Japan.

編集兼発行　日本原子力研究所
印　　刷　日青工業株式会社

JAERI-M 86-017

Current Generation by a Large Amplitude Wave Packet

Shoji TANAKA*

Department of Large Tokamak Research,
NAKA Fusion Research Establishment
Japan Atomic Energy Research Institute
Naka-machi, Naka-gun, Ibaraki-ken

(Revised January 29, 1986)

Nonlinear electron dynamics in a large amplitude wave packet with coherent structure is investigated via Fokker-Planck equations and mapping equations from the viewpoint of toroidal current generation in tokamak plasmas. Electrons are trapped (and detrapped) by the coherent wave potential whose amplitude is large so that the electron bounce time in the wave potential is smaller than the electron transit time through the packet. This effect is now included into the wave-induced friction and diffusion terms in the Fokker-Planck equation. The quasi-steady state distribution function of electrons is obtained to have a tail which is neither a quasilinear one nor a plateau. The wave induced current, the dissipated power, and their ratio are numerically calculated to be compared to those obtained from the quasilinear theory.

Keywords: RF Current Generation, Coherent Wave Packet, Nonlinear Electron Dynamics, Mapping Equations, Stochasticity, Fokker-Planck Equations.

---

* On leave from Nagoya University.
Present address: Department of Electrical and Eletronics Engineering, Sophia University, Tokyo 102.

JAERI-M 86-017

大振幅波束による電流生成

日本原子力研究所那珂研究所臨界プラズマ研究部
田中　昌司*

（1986年1月29日受理）

トカマク・プラズマにおけるトロイダル電流生成の観点から，コヒーレントな大振幅波束中の電子の非線形運動を，フォッカー・プランク方程式及びマッピング方程式を用いて解析した。波束の振幅が大きく，波のポテンシャル中の電子のバウンス時間が電子の波束通過時間より短い場合は，ポテンシャルによって電子が補捉（及び脱補捉）される。この効果をフォッカー・プランク方程式の，波動による摩擦項と拡散項に取り入れ，電子の準定常分布関数を求めた。波束によって生成される電流，散逸パワー，及びそれらの比を求めて，準線形理論から得られるものと比較した。

那珂研究所：茨城県那珂郡那珂町大字向山
＊　核融合特別研究生：名古屋大学工学部
現在：上智大学理工学部電気電子工学科

Contents

目　　次

1. Introduction

Evolution of plasmas interacting with small amplitude wave packets is described by the quasi-linear theory (QLT).[1-6] In this theory, the lowest order distribution function is changed by higher order fluctuations through diffusion processes. It is limited for the rather weak field case, $\sqrt{\alpha}\tau < 1$ ($\sqrt{\alpha}$: the normaized bounce frequency of particles in the wave potential, τ: the normalized auto-correlation time of the wave) to validate this theory.

When the wave amplitude becomes larger ($\sqrt{\alpha}\tau > 1$), particle trapping by the wave potential begins to occur, which QLT does not take into account. As a result, the diffusion coefficient of the particle in velocity space, for example, is no longer proportional to the square of the wave amplitude as QLT shows. Many researchers have been investigated this feature by test particle studies in turbulent wave packets.[7-10] And theoretical studies have been made in order to describe the wave-particle interaction in rather strong wave fields.[11-13] Especially the theories in Refs. 11 and 12 are well-known as the Dupree-Weinstock theory or the resonance broadenig theory.

Concerning particle dynamics in finite-amplitude monochromatic waves, on the other hand, the work of O'Neil[14] is widely known. Since this is done in the framework of the Vlasov theory, that is, Coulomb collisions are not included in this theory, trapped/untrapped orbits are well-defined. The inclusion of slight collisions have been accomplished by Zakharov and Karpman[15] and Sugihara *et al.*[16] for electrostatic waves.

In the field of fusion research, considerable interest has been paid for generating toroidal currents in tokamak plasmas with radio frequaency (RF) waves recently. In particular, the idea of current drive by lower hybrid waves (LHW's)[17] has been confirmed by many experiments.[18] In the practical situatin of LHW current drive and also heating, the externally launched LHW usually propagates along a resonance cone, in which the wave forms a coherent wave packet. Because the amplitude of LHW is large for the practical incident wave power (typically, $E \sim 10^2\ kV/m$ in recent experiments), QLT may be inapplicable although many works have been done in the framework of QLT. It is therefore necessary to investigate electron dynamics in coherent wave packets whose amplitudes are beyond the QL limit, $\sqrt{\alpha}\tau > 1$.

The purpose of the present paper is to investigate electron dynamics in such coherent RF wave packets, especially for the wave amplitudes which are beyond the QL limit, from the viewpoint of toroidal current generation in tokamak plasmas. The method employed here is the *perturbed-orbit method*,[19-21] in which the first and the second moments of particle velocity changes are calculated to be included into a Fokker-Planck equation. The resultant equation coincides with that obtained in QLT when the wave amplitude is small ($\sqrt{\alpha}\tau < 1$). This formulation has the advantage that the employing phase averaging makes unnecessary any averaging over an ensemble of fluctuation fields. Therefore this formulation is applicable to situations involving highly coherent wave fields.

The Fokker-Planck equation which includes the effects of electron trapping by the wave potential will be write down within

the framework of the above formulation. The current induced by the wave field, the power dissipated into the plasma, and their ratio will be calculated numerically from the quasi-steady state distribution function obtained from the Fokker-Planck equation. They will be compared to those obtained from QLT. This paper is organized as follows: In § 2 we derive the QL diffusion equation assuming that the wave amplitude is small. We integrate the equations of motion in § 3 in order to derive the first and the second moments of the velocity variation for the arbitary amplitude waves. Mapping results are presented in § 4 in order to grasp the intrinsic nature of electron motion in the coherent wave packets with various amplitudes. § 5 is devoted to the Fokker-Planck description of the electron dynamics for large amplitude waves. Summary is given in § 6.

2. Quasilinear Theory

As a representation of a coherent wave packet, let us consider the wave packet which is defined by

$$E(X,T) = E\sin(kX-\omega T+\varphi), \qquad 0 \leqq X \leqq l, \tag{1a}$$

$$0, \qquad elsewhere, \tag{1b}$$

where E is the strength of the electric field of the wave packet and k (ω) is the wavenumber (frequency) of the carrier wave. The equations of motion of electrons in the wave packet are written as

$$\dot{x} = v - 1, \tag{2}$$

$$\dot{v} = -\alpha\sin(x+\varphi), \tag{3}$$

where $x = kX-\omega T$, $\dot{x} = dx/dt$, $t = \omega T$, $\alpha = keE/m_e\omega^2 = \omega_b^2/\omega^2$, e (m_e) the charge (mass) of the electron.

In the present section, we assume that the wave amplitude is small ($\alpha \ll 1$), and derive the quasilinear diffusion equation in velocity space. Eq. (3) is expanded perturbatively with the smallness parameter α to give

$$\dot{v}_0 = 0, \tag{4}$$

$$\dot{v}_1 = -\alpha\sin[(v_0-1)t+\varphi], \tag{5}$$

$$\dot{v}_2 = -\alpha\int_0^t v_1(t')dt'\cos[(v_0-1)t+\varphi], \tag{6}$$

from which the velocity of the particle is obtained to be

$v = v_0+v_1+v_2+\cdots$. The condition of divergence of this series gives the validity condition of QLT as $\sqrt{\alpha}\tau < 1$. The transit time of the particle through the wave packet, τ, is defined by

$$kl = \int_0^\tau \{v_0+v_1(t)+\cdots\}dt. \tag{7}$$

Up to the first order in α, τ is expressed as $\tau = \tau_0+\Delta\tau+O(\alpha^2)$, where

$$\tau_0 = \frac{kl}{v_0}, \tag{8}$$

$$\Delta\tau = -\frac{\alpha}{v_0(v_0-1)^2}\{\sin[(v_0-1)\tau_0+\varphi]-\sin\varphi-(v_0-1)\tau_0\cos\varphi\}. \tag{9}$$

Then the variation of the particle velocity by passing through the wave packet is given by

$$\begin{aligned}\Delta v &= \int_0^\tau \{\dot{v}_1(t)+\dot{v}_2(t)+\cdots\}dt \\ &= \frac{\alpha}{v_0-1}\{\cos[(v_0-1)\tau_0+\varphi]-\cos\varphi\} \\ &\quad -\frac{\alpha^2}{(v_0-1)^3}\{\cos[(v_0-1)\tau_0+\varphi]-\cos\varphi\}\cos[(v_0-1)\tau_0+\varphi] \\ &\quad -\frac{\alpha^2}{v_0(v_0-1)^3}\{\sin[(v_0-1)\tau_0+\varphi] \\ &\qquad -\sin\varphi-(v_0-1)\tau_0\cos\varphi\}\sin[(v_0-1)\tau_0+\varphi] \\ &\quad +O(\alpha^3).\end{aligned} \tag{10}$$

Randomness of particle orbits is essential in QLT. Then we require in our formulation that there exists a decorrelation mechanism in particle motion; slight Coulomb collisions are enough to yield decorrelated particle motion, which will be

argued on later, and also the nonlinear equations (2) and (3) themselves may have intrinsic stochastisity (§ 4). Then, taking the ergodic hypothesis, we replace the average along the stochastic orbit by the average on the random initial phases which is defined by

$$< > = \frac{1}{2\pi}\int_{-\pi}^{\pi} d\varphi. \tag{11}$$

The mean deviation and the mean square deviation of the particle velocity are obtained as

$$<\Delta v> = -\frac{\alpha^2}{2}\left[\frac{v_0+1}{v_0(v_0-1)^3}\{1-\cos[(v_0-1)\tau_0]\}\right.$$

$$\left.+\frac{kl}{v_0^2(v_0-1)^2}\sin[(v_0-1)\tau_0]\right] + O(\alpha^3) \tag{12}$$

and

$$<(\Delta v)^2> = \frac{\alpha^2}{(v_0-1)^2}[1-\cos[(v_0-1)\tau_0]\} + O(\alpha^3). \tag{13}$$

In the following, we simply write v_0 as v.

In a toroidal plasma with periodicity of length $2\pi R$ (R is the major radius of the torus), electrons pass through the wave packet repeatedly with time intervals of $\Delta t = 2\pi kR/v$. If there were no Coulomb collision between the particles, they would see the wave packet composed of discrete muliti-modes because the system is periodic. But there exists Coulomb collisions in practical plasmas. Now let us ask how the particles see the packet. The interval in wave number space between the adjacent modes of the packet in the periodic system is $\delta k \sim R^{-1}$. This means that the phase velocities of them have a difference of $\delta(\omega/k) \sim \omega/k^2R$. On the other hand, the spread of electron

velocity due to Coulomb collisions is $\delta V \sim (2\pi RV/\tau_c)^{1/2}$ during a circulation of the torus, where τ_c is the collision time. With the typical parameters of $\omega = 2\pi\times10^9$ s^{-1}, $k = 100$ m^{-1}, $R = 1$ m, $V = 2\pi\times10^7$ m/s and $\tau_c = 1\times10^{-4}$ s, we can estimate as $\delta(\omega/k) \sim 2\pi\times10^5$ m/s and $\delta V \sim 2\pi\sqrt{10}\times10^5$ m/s. Therefore we may understand that the particles see the packet with a continuous spectrum. It may be said that the particles lose the memory of the motion by Coulomb collisions during circulating the torus so that they forget that the system is periodic. Then we may be able to use the expressions of the velocity changes (Eqs. (12) and (13)) which are obtained for the wave packet with the continuous spectrum. And the particle dynamics is described by the Fokker-Planck equation with the coefficients obtained from Eqs. (12) and (13).

The Fokker-Planck equation is generally written by

$$\frac{\partial f}{\partial t} = -\frac{\partial}{\partial v}(Ff) + \frac{\partial^2}{\partial v^2}(Df), \tag{14}$$

where $f = f(v,t)$ is the electron distribution function in velocity space and

$$F = \frac{<\Delta v>}{\Delta t} = \frac{l}{2\pi R}\frac{<\Delta v>}{\tau} \tag{15}$$

and

$$D = \frac{<(\Delta v)^2>}{2\Delta t} = \frac{l}{2\pi R}\frac{<(\Delta v)^2>}{2\tau} \tag{16}$$

are the friction and the diffusion coefficients. Using Eqs. (12) and (13) for $<\Delta v>$ and $<(\Delta v)^2>$ in the above equations, we recognize that the relation,

$$F = \frac{\partial D}{\partial v}, \tag{17}$$

is hold. In other words, the difference between F and $\partial D/\partial v$ is as small as $O(\alpha^3)$. Then we get the QL diffusion equation,

$$\frac{\partial f}{\partial t} = \frac{\partial}{\partial v} D \frac{\partial f}{\partial v}. \tag{18}$$

The distribution function in quasi-steady state is obtained from the Fokker-Planck equation,

$$\frac{\partial f}{\partial t} = \frac{\partial}{\partial v} D \frac{\partial f}{\partial v} + C_e(f), \tag{19}$$

where

$$C_e(f) = C_{ee}(f) + C_{ei}(f) \tag{20}$$

is the linearized one-dimensional collision operator. Defining the collision frequency as

$$\nu_p = \frac{e^4 n_e \ln\Lambda}{\pi \varepsilon_0^2 m_e^2} \frac{1}{\omega} \left(\frac{k}{\omega}\right)^3, \tag{21}$$

where n_e is the electron density and $\ln\Lambda$ is the Coulomb logarithm, we can write down the collision operator as

$$C_e(f) = \frac{3}{2} \nu_p \frac{\partial}{\partial v} \frac{1}{v^3} \left(vf + v_t^2 \frac{\partial f}{\partial v}\right), \tag{22}$$

where $v_t = k\sqrt{T_e/m_e}/\omega$ is the electron thermal velocity normalized to the phase velocity of the carrier wave and $Z = 1$ for the background ions is assumed for simplicity. This collision operator is applicable for $v_t \ll 1$ as in the present case. Since we are interested in the time scale which is much longer than the circulation time of the electrons around the torus but much shorter than the heating time of the bulk electrons, we here assume that the bulk temperature is constant. Thus obtained

quasi-steady state solution to Eq. (19) is given by

$$f(v) = C_0 \exp\left\{-\int_0^v \frac{3\nu_p v/2}{3\nu_p v_t^2/2 + v^3 D} dv\right\}, \tag{23}$$

where C_0 is the normalization constant.

In Fig. 1, the diffusion coefficient (16) is depicted. And the distribution function (23) is shown in Fig. 2. The parameters are chosen as $v_t = 0.25$, $\nu_p = 1.6\times10^{-6}$, $kl = 20.0$, $n_e = 5\times10^{19}$ m^{-3}, and $\ln\Lambda = 16$, and the others are the same as those given earlier. The power spectrum of the present wave packet, $S(v)$, is given by

$$S(v) = \alpha^2 \left(\frac{kl}{2\pi}\right)^2 \frac{\sin^2(kl(v-1)/2v)}{(kl(v-1)/2v)^2}. \tag{24}$$

The diffusion coefficient is connected with the power spectrum by the relation,

$$D(v) = \frac{\pi}{2kR}\frac{S(v)}{v}, \tag{25}$$

which is easily seen from Eqs. (13), (16), and (24). The relation (17) and (25) are well-known results of QLT. Because of the relation (25), the profile of D_{QL} is invariable as far as the wave amplitude is small ($\sqrt{\alpha} < 1$). It will be shown in § 5 that these relations are not hold when the wave amplitude is larger ($\sqrt{\alpha}\tau > 1$).

3. Integration of the Equations of Motion

Eqs. (2) and (3) are integrated to give

$$\dot{x} = 2\sigma\sqrt{\alpha}\,\{\beta^2-\sin^2[(x+\varphi)/2]\}^{1/2}, \tag{26}$$

where $\sigma = \mathrm{sgn}(\dot{x})$, $\beta^2 = W/2\alpha$, and $W = \dot{x}^2/2+\alpha[1-\cos(x+\varphi)]$.

Now the particles are devided into two groups; the trapped particles ($\beta^2 < 1$) and the untrapped particles ($\beta^2 > 1$).

i) *Trapped particles.*

Further integration of Eq. (26) gives

$$\sqrt{\alpha}\,(t+t_0) = \int_0^z \frac{dz}{(1-z^2)^{1/2}(1-\beta^2z^2)^{1/2}} = sn^{-1}z \tag{27}$$

$$\leftrightarrow \quad z = sn[\sqrt{\alpha}\,(t+t_0);\beta], \tag{28}$$

where $sn[\alpha(t+t_0);\beta]$ is the Jacobi elliptic sn function with the argument $\sqrt{\alpha}\,(t+t_0)$ and the modulus of β, $\beta z = \sin[(x+\varphi)/2]$, and $t_0 = \{t;\ \sin(\varphi/2) = \beta sn(\sqrt{\alpha}\,t;\beta)\}$. We then obtain the integratin of motion for the trapped particles as

$$\sin\frac{x+\varphi}{2} = \beta sn[\sqrt{\alpha}\,(t+t_0);\beta]. \tag{29}$$

ii) *Untrapped particles.*

From Eq. (26), we get

$$\beta\sqrt{\alpha}\,(t+t_0) = \sigma\int_0^z \frac{dz}{(1-z^2)^{1/2}(1-z^2/\beta^2)^{1/2}} = \sigma sn^{-1}z \tag{30}$$

$$\leftrightarrow \quad z = \sigma sn[\beta\sqrt{\alpha}\,(t+t_0);\beta^{-1}], \tag{31}$$

where $z = \sin[(x+\varphi)/2]$ and $t_0 = \{t;\ \sin(\varphi/2) = \sigma sn(\beta\sqrt{\alpha}\,t;\beta^{-1})\}$. Then the integratin of motion for the untrapped particles is

$$\sin\frac{x+\varphi}{2} = \sigma sn\left[\beta\sqrt{\alpha}\,(t+t_0);\beta^{-1}\right] . \tag{32}$$

On the contrary to the trapped particle case, σ cannot be eliminated from the above equations. This is because the $\sigma = +1$ particles and the $\sigma = -1$ particles are well distinguished for the untrapped case.

From Eqs. (29) and (32), the velocities of the particles ($v = 1+dx/dt$) are given as

$$v^{TP}(t) = 1 + 2\beta\sqrt{\alpha}\,cn\left[\sqrt{\alpha}\,(t+t_0);\beta\right] , \tag{33}$$

$$v^{UT}(t) = 1 + 2\sigma\beta\sqrt{\alpha}\,dn\left[\beta\sqrt{\alpha}\,(t+t_0);\beta^{-1}\right] , \tag{34}$$

where TP (UT) denotes trapped (untrapped) particles, and cn and dn are Jacobi elliptic functions. The velocity changes of the particles passing through the wave packet, $\Delta v = v(\tau)-v(0)$, are

$$\Delta v_{\pm}^{TP}(t_0) = 2\beta\sqrt{\alpha}\left\{cn\left[\sqrt{\alpha}\,(t_0\pm\tau);\beta\right]-cn(\sqrt{\alpha}\,t_0;\beta)\right\} , \tag{35}$$

$$\Delta v_{\pm}^{UT}(t_0) = 2\sigma\beta\sqrt{\alpha}\left\{dn\left[\beta\sqrt{\alpha}\,(t_0\pm\tau);\beta^{-1}\right]-dn(\beta\sqrt{\alpha}\,t_0;\beta^{-1})\right\} , \tag{36}$$

where t_0 is the time when the particle enters the packet, and signs are identical to those of x. The transit time through the packet, τ, is obtained from

$$kl = \int_0^{\tau}\left[1+2\beta\sqrt{\alpha}\,cn(\sqrt{\alpha}\,t;\beta)\right]dt \tag{37}$$

for the trapped particles, and from

$$kl = \int_0^{\tau}\left[1+2\sigma\beta\sqrt{\alpha}\,dn(\beta\sqrt{\alpha}\,t;\beta^{-1})\right]dt \tag{38}$$

for the untrapped particles. Note the parities of Δv and φ,

which are

$$\Delta v_-(t_0) = \Delta v_+(-t_0), \tag{39}$$

$$\varphi(t_0) = -\varphi(-t_0) \geqq 0, \qquad \varphi(0) = 0. \tag{40}$$

Now we obtain the first and the second moment of Δv by the phase average (11). Using Eqs. (35) and (36), we get

$$\begin{aligned}
\langle \Delta v \rangle &= \frac{1}{2\pi}\int_0^{\varphi_1} [\Delta v_+^{TP}(t_0) + \Delta v_-^{TP}(t_0)]\, d\varphi \\
&\quad + \frac{1}{2\pi}\int_{\varphi_1}^{\pi} [\Delta v_+^{UT}(t_0) + \Delta v_-^{UT}(t_0)]\, d\varphi \\
&= \frac{\sqrt{\alpha}}{\pi}\int_0^{t_1} \beta\, [c(\tau,\beta) + c(-\tau,\beta) - 2c(0,\beta)]\, \frac{d\varphi}{dt_0} dt_0 \\
&\quad + \frac{\sqrt{\alpha}}{\pi}\int_{t_1}^{K(\beta^{-1})/\beta\alpha^{1/2}} \beta\, [d(\tau,\beta^{-1}) + d(-\tau,\beta^{-1}) - 2d(0,\beta^{-1})]\, \frac{d\varphi}{dt_0} dt_0
\end{aligned} \tag{41}$$

and

$$\begin{aligned}
\langle (\Delta v)^2 \rangle &= \frac{1}{2\pi}\int_0^{\varphi_1} \{ [\Delta v_+^{TP}(t_0)]^2 + [\Delta v_-^{TP}(t_0)]^2 \}\, d\varphi \\
&\quad + \frac{1}{2\pi}\int_{\varphi_1}^{\pi} \{ [\Delta v_+^{UT}(t_0)]^2 + [\Delta v_-^{UT}(t_0)]^2 \}\, d\varphi \\
&= \frac{2\alpha}{\pi}\int_0^{t_1} \beta^2 \{ [c(\tau,\beta) - c(0,\beta)]^2 \\
&\qquad + [c(-\tau,\beta) - c(0,\beta)]^2 \}\, \frac{d\varphi}{dt_0} dt_0 \\
&\quad + \frac{2\alpha}{\pi}\int_{t_1}^{K(\beta^{-1})/\beta\alpha^{1/2}} \beta^2 \{ [d(\tau,\beta^{-1}) - d(0,\beta^{-1})]^2 \\
&\qquad + [d(-\tau,\beta^{-1}) - d(0,\beta^{-1})]^2 \}\, \frac{d\varphi}{dt_0} dt_0,
\end{aligned} \tag{42}$$

where $K(\beta^{-1})$ is the complete elliptic integral of the first kind,

$t_1 = \{t;\ \sin(\varphi_1/2) = sn(\sqrt{\alpha}\, t; 1)\}$, $\qquad \varphi_1 = \{\varphi;\ \beta = \beta(v, \varphi; t=0) = 1\}$

(see Fig. 3), and the abbreviations,

$$c(\tau,\beta) = cn[\sqrt{\alpha}(t_0+\tau);\beta], \tag{43}$$

$$d(\tau,\beta^{-1}) = dn[\beta\sqrt{\alpha}(t_0+\tau);\beta^{-1}], \tag{44}$$

have been used.

Right hand sides (RHS's) of Eqs. (41) and (42) are the functions of v, which are plotted in Figs. 4, 5, 6, and 7. The bars in the figure indicate the trapping regions, $1-2\sqrt{\alpha} \leqq v \leqq 1+2\sqrt{\alpha}$, where $2\sqrt{\alpha}$ is the trapping velocity. In Figs. 5, 6, and 7, the mean square deviation of the particle velocities (43) is caved around the resonance velocity ($v = 1$) by particle trappins. This effects are remarkable when $\sqrt{\alpha}\tau > \pi$. This condition coincides with that the trapping velocity exceeds the spread of the wave spectrum, $2\pi/kl$.

In Fig. 8, $<(\Delta v)^2>$ for the resonance particles ($v = 1$) is plotted as a function of α. Substituting $v = 1$ in Eq. (42), we obtain

$$<(\Delta v)^2>|_{v=1} \fallingdotseq \frac{1}{2}\alpha^2\tau^2 \tag{45}$$

for $\sqrt{\alpha}\tau \ll 1$, and

$$<(\Delta v)^2>|_{v=1} \fallingdotseq \alpha \tag{46}$$

for $\sqrt{\alpha}\tau \gg 1$, Eq. (45) should coincide with the results obtained from QLT; indeed Eq. (13) gives $<(\Delta v)^2>_{QL} = \alpha^2\tau^2/2$ for $v_0 = 1$. The quantity, $<(\Delta v)^2>|_{v=1}/<(\Delta v)^2>_{QL}$, calculated from Eq. (42) is plotted in Fig. 9. Though the condition $\sqrt{\alpha}\tau \ll 1$ is necessary to derive Eq. (45), numerical calculation of Eq. (42) shows that it holds for $\sqrt{\alpha}\tau < 1$. For $\sqrt{\alpha}\tau > 2\pi$, numerical results coincide

with Eq. (46). Noting that $\sqrt{\alpha}\tau = 2\pi\tau/\tau_b$, where $\tau_b = 2\pi\omega/\omega_b$ is the particle bounce time normalized to the wave oscillation period, we rewrite this condition as $\tau/\tau_b > 1$. This means that the numerical results fit Eq. (46) when the particle transit time through the wave packet is larger than the particle bounce time. In Fig. 8, the effect of particle bouncing appears around $\alpha \sim 10^{-1}$, although the origin of the ripples for $\alpha > 10$ is not clear.

4. Mapping Equations

In this section, we investigate nonlinear electron dynamics via mapping equations. The present system has a periodicity in the toroidal direction as is stated earlier. Then the particle motion is described by discrete variables with the interval of the periodicity of the system. Sampling the particle motion at a certain poloidal cross section, we obtain the time series of $\{v_j, \varphi_j\}$ $(j = 0,1,2, \ldots)$. Here φ_j is the wave phase at an entrance of the packet. This discrete stochastic process is defined by the mapping equations,

$$v_{j+1} - v_j = \Delta v_{j+1}, \tag{47a}$$

$$\varphi_{j+1} - \varphi_j = \Delta \varphi_{j+1}. \tag{47b}$$

From Eqs. (35) and (36), we write down RHS of Eq. (47a) as

$$\Delta v^{TP}_{\pm,j+1} = 2\beta_j\sqrt{\alpha}\,\{cn[\sqrt{\alpha}\,(t_j \pm \tau_j);\beta_j] - cn(\sqrt{\alpha}\,t_j;\beta_j)\} \tag{48a}$$

for the trapped particles and

$$\Delta v^{UT}_{\pm,j+1} = 2\sigma\beta_j\sqrt{\alpha}\,\{dn[\beta_j\sqrt{\alpha}\,(t_j \pm \tau_j);\beta_j^{-1}] - dn(\beta_j\sqrt{\alpha}\,t_j;\beta_j^{-1})\} \tag{48b}$$

for the untrapped particles, where the signs are those of φ_j, and

$$\beta_j = \beta_j(v_j, \varphi_j) = \left[\left(\frac{v_j}{2\alpha^{1/2}}\right)^2 + \sin^2\frac{\varphi_j}{2}\right]^{1/2}, \tag{49}$$

$$t_j = \left\{t;\ \sin\frac{\varphi_j}{2} = \beta_j sn(\sqrt{\alpha}\,t;\beta_j)\ for\ TP,\right.$$

$$\left.\sin\frac{\varphi_j}{2} = \sigma sn(\beta_j\sqrt{\alpha}\,t;\beta_j^{-1})\ for\ UT\right\}, \tag{50}$$

$$\tau_j = \frac{k\,l}{v_j}. \tag{51}$$

RHS of Eq. (47b) is written as

$$\Delta\varphi_{j+1} = k\left(2\pi R - \frac{l}{v_j} - \frac{2\pi R - l}{v_{j+1}}\right). \tag{52}$$

The mapping equations (47) have a periodicity in $\varphi_j \in [-\pi, \pi]$ and are inhomogeneous in $v_j \in (-\infty, \infty)$.

The time series of $\{v_j\}$ $(j = 0,1,2, \ldots)$ obtained numerically from Eqs. (47) are shown in Figs. 10 for (a) $\alpha = 5.0\times10^{-6}$ $(\sqrt{\alpha}\,\tau_0 = 0.04472,\ \tau_0 = 20.0)$, (b) 1.0×10^{-3} (0.6323), (c) 5.625×10^{-3} (1.50), and (d) 3.0×10^{-2} (3.464). The parameters used in the above equations are the same in § 2. Regular motion is seen in Fig. (a). There is a threshold of $\sqrt{\alpha}\,\tau$ above which the particle motion bocomes stochastic; the quantity 0.04472 may be below the threshold, which will be evaluated later with a reduced standard mapping. Random walk is seen in Figs. (b) and (c). The dashed lines indicate the trapping region. In the case of (c), the steps of the random walk are larger than those in (b), although the steps outside the trapping region remain small (iteration number 81-87, 147-161, and 185-191). This is because the diffusion coefficients are extended in the trapping region for about $\sqrt{\alpha}\,\tau > 1.5$, as is seen in Fig. 5 (b).

On the contrary, the motion in (d) is no longer a random walk in the trapping region. This strongly reflects the trapping effect by the wave potential. Outside the trapping region, however, the motion is still a random walk (iteration number 73-109). In this case, the velocity change in the trapping region is of the order of the trapping velocity ($\Delta v \sim 2\sqrt{\alpha}$).

In particular situation, Eqs. (47) are reduced to the standard mapping,[22] which has been investigated well. Leaving the derivation to the Appendix, we here write down the result,

$$\tilde{v}_{j+1} - \tilde{v}_j = A\sin\tilde{\varphi}_j, \tag{53a}$$

$$\tilde{\varphi}_{j+1} - \tilde{\varphi}_j = \tilde{v}_{j+1}, \tag{53b}$$

where $\tilde{v}_j = \pi kR\,[v_j + v_0(v_0-2)]/v_0^2$, $\tilde{\varphi}_j = \varphi_j/2$, and $A = (\pi R/l v_0)\alpha\tau_0^2$. The threshold of A for the particle motion being stochastic is given by the Chirikov condition,[22] $A > 1$. In the present case, this leads $\sqrt{\alpha}\tau_0 > 0.25$ for $v_0 = 1$, which is consistent with the results of the mapping (47). The standard mapping (53) does not describe the particle trapping; the particles diffuse when $A > 1$. In the limit of $A \to \infty$, the particle motion is completely decorrelated. Then the diffusion coefficient is obtained as

$$D_{SM} = \langle(\tilde{v}_{j+1}-\tilde{v}_j)^2\rangle = A^2/2, \tag{54}$$

where $\langle\ \rangle$ is the average over $\tilde{\varphi}_j$. From the last section, we see that it is identical to the QL diffusion coefficient for the resonance particles ($v = 1$). Then it coincides with that of the original mapping (47) for the resonance particles when $\sqrt{\alpha}\tau \ll 1$.

5. Fokker-Planck Equation in the Nonlinear Regime

When the wave amplitude is large ($\sqrt{\alpha}\tau > 1$), electrons are trapped (and detrapped) by the coherent wave potential. In order for the Fokker-Planck description is valid, the trapping velocity, $2\sqrt{\alpha}$, must be smaller than the spread of the wave spectrum, $2\pi/kl$; otherwise the velocity changes are so large that it is not be able to define the Fokker-Planck coefficients which are local in velocity space. Then there exists an upper limit of the wave amplitude for the validity of the Fokker-Planck description, $\sqrt{\alpha}\tau < \pi\tau/kl \fallingdotseq \pi$ ($\tau \fallingdotseq kl = 20$ in the present case). Within the limit, the particle dynamics is described by the Fokker-Planck equation with the coefficients (15) and (16) in which $<\Delta v>$ and $<(\Delta v)^2>$ are substituted from Eqs. (41) and (42):

$$\frac{\partial f}{\partial t} = -\frac{\partial}{\partial v}\left[\left(F-\frac{\partial D}{\partial v}\right)f\right] + \frac{\partial}{\partial v}D\frac{\partial f}{\partial v} + C_e(f). \tag{55}$$

This equation includes the effects of particle trapping. The quasi-steady state distribution function is given by

$$f(v) = C_0 \exp\left\{-\int_0^v \frac{3\nu_p v/2 - v^3(F-\partial D/\partial v)}{3\nu_p v_t^2/2 + v^3 D}dv\right\}. \tag{56}$$

Contrary to QLT, $F-\partial D/\partial v$ is not vanishing for the wave amplitude, $1 < \sqrt{\alpha}\tau < \pi$. These features will be investigated in the following. In Figs. 11 and 12 shown are the Fokker-Planck coefficients which are given by Eqs. (15), (16), (41), and (42) for the two cases of $\sqrt{\alpha}\tau = 1.0$ (Fig. 11) and 2.0 for $\tau = 20$ (Fig. 12). On the contrary to the former case, a glance shows that $F = \partial D/\partial v$ does not hold in the latter case. The more quantitavie feature is shown in Figs. 13, 14, and Table I. Since

$v \sim 1$, the magnitude of $v^3(F-\partial D/\partial v)$ in Eq. (56) is about 6×10^{-7} in the former case and 4×10^{-5} in the latter case. Using the same parameters mentioned in the last section, we estimate that $3\nu_p v/2 \sim 2\times10^{-6}$. Therefore $v^3(F-\partial D/\partial v)$ can be neglected in the former case, which is consistent with QLT. In the latter case, however, the term of $v^3(F-\partial D/\partial v)$ may play important role.

In Fig. 15 and 16, the quasi-steady state distribution function $f(v)$ given by Eq. (56) is shown for the above two cases. The high energy tail in Fig. 15 bears close resemblence to that obtained in QLT (Fig. 2). The more enhanced tail is shown in Fig. 16. In this case $f(v)$ is no longer a monotonically decreasing function of v, and neither does form a plateau. This is caused by the $F-\partial D/\partial v$ term. Note that, in the figure, the acceleration phase in velocity space, $F-\partial D/\partial v > 0$, and the deceleration phase, $F-\partial D/\partial v < 0$, correspond to the humps of the tail.

The current induced by the wave packet is calculated from

$$J = \int_{-\infty}^{\infty} v f(v) dv, \tag{57}$$

and the power dissipated into the plasma is calculated from

$$P_d = \frac{1}{2}\int_{-\infty}^{\infty} v^2 \frac{\partial}{\partial v}\left[-\left(F-\frac{\partial D}{\partial v}\right)f(v)+D\frac{\partial f(v)}{\partial v}\right] dv. \tag{58}$$

The induced currents are plotted in Fig. 17. The broken line is that calculated from QLT (Eqs. (23) and (57)). The solid line is that obtained in the present section (Eqs. (56) and (57)). For $\alpha < 2.5\times10^{-3}$ ($\sqrt{\alpha}\tau < 1$), both lines are close. This means that J of the solid line is almost proportional to α^2. It shows the tendency of transition to be proportional to α for larger α's. The similar results are obtained for the dissipated powers, which

are plotted in Fig. 18. An important quantity in arguing about RF current drive is the ratio of the induced current, J, to the deposited power, P_d; that is, J/P_d. It is obtained from the distribution function (56) and is shown in Fig. 19 as a function of α. Their dependence on α are rather weak, although J and P_d increase with increasing α. The ratio obtained in the present section is a little larger than that obtained in QLT.

6. Summary

In the present paper, we have write down two types of Fokker-Planck equations which describe electron dynamics in a model wave packet. First, the so-called QL equation has been obtained, which is valid for small amplitude wave packets ($\sqrt{\alpha}\tau < 1$). Second, derived has been the Fokker-Planck equation which includes the effect of particle trapping by the wave potential. This description is applicable even for larger amplitude wave packets ($\sqrt{\alpha}\tau < \pi$). The quasi-steady state distribution functions of electrons have been obtained from the equations. The distribution function for the large amplitude case has a tail which is neither a QL one nor a plateau. The current induced by the wave field and the ratio of the current to the dissipated power have been calculated numerically with the distribution functions. Comparison has been made between the electron distribution functions, the wave induced currents, etc. those obtained from the two theories. For the small amplitude wave packet ($\sqrt{\alpha}\tau < 1$), the induced current is almost proportional to the square of the amplitude as in QLT. It switches to be proportional to the amplitude for the large amplitude case ($\sqrt{\alpha}\tau > 1$). The ratio of the induced current to the dissipated power calculated from the latter theory is almost the same as or a little greater than that calculated from QLT.

The method of formulation employed in the present paper is the perturbed-orbit method. This formulation has the advantage that the employing phase averaging makes unnecessary any averaging over an ensemble of fluctuation fields. Then this

formulation is suitable for highly coherent fields like the present case. In the case of the weak wave fields, the resultant equation coincides with that obtained in QLT. Note that the QL diffusion equation describes the diffusion of resonance particles. The perturbed-orbit method formulates the dynamics of resonence particles; the contribution from nonresonance particles is excluded. Only the diffusion of the resonence particles is the true one, which is an irreversible process. The response of nonresonance particles, which is a reversible process, is related to the change in wave amplitudes,[15] and this is not the present case.

Decorrelation mechanism is essential for the Fokker-Planck description. We have recognized in § 2 that slight Coulomb collisions are enough to yield stochastic particle motion. The Coulomb collisions are necessary also to yield quasi-steady state distribution functions, which are generally given by Eq. (56). The wave produced tail of the distribution function which is a monotonically decreasing function of v is formed when the wave term, $v^3(F-\partial D/\partial v)$, is neglected compared to the collision term, $3\nu_p v/2$, in Eq. (56) because of the monotonicity of the collision term (Fig. 15). On the other hand, the tail which is not a monotonically decreasing function of v is formed when the wave term dominates the collision term because of the non-monotonicity of the wave term (Fig. 16). From the Table and remembrance of $3\nu_p v/2 \sim 2\times10^{-6}$ in our case, we see that the criterion of the wave amplitude distinguishing the two cases is $\sqrt{\alpha}\tau \sim 1$. This coinsides with that distinguishing the QL regime and the nonlinear regime in the present case,

Even if Coulomb collisions are absent, electron motion can be stochastic for some magnitudes of the wave amplitudes, because the nonlinear equations of motion (2) and (3) have intrinsically stochastic nature. The mapping equations which describe the electron dynamics have been obtained in order to investigate the intrinsic nature. Some examples of the numerical solutions have been presented. The motion is stochastic when the wave apmlitude exceeds a certain value. However, the motion is no longer stochastic for the very large amplitude waves ($\sqrt{\alpha}\tau > \pi$) due to strong trapping by the wave potential. In particular situation, the mapping equations could be reduced to the standard mapping form. This gives the stochastic threshold of the wave amplitude. The diffusion coefficient obtained from the standard mapping coincides with that obtained from the original mapping for $\sqrt{\alpha}\tau \ll 1$.

The model wave packet employed in the present paper is an idealized one. The wave amplitude is constant in time. The wave field is coherent. And the profile of the envelope of the packet is rectangular. But this is not necessarily unpractical for the LH current drive; the wave field is in a steady state with a coherent structure and the waves are usually launched by waveguide antennas with rectangular cross sections.

There is an upper limit of the wave amplitude for the Fokker-Planck description as is already mentioned earlier ($\sqrt{\alpha}\tau < \pi$). When the wave amplitude exceeds the limit, the electrons suffer nonlocal scattering by the wave packet because the trapping velocity is greater than the spread of the wave spectrum, $2\sqrt{\alpha} > 2\pi/kl$. This feature is seen in Fig. 10 (d). The

scattering is no longer a diffusion process which is local in velocity space, and the electron motion may become similar to that in a monochromatic wave due to the deep trappig by the wave potential. Further study is in progress to investigate such highly nonlinear electron motion.

Acknowledgements

This work has been accomplished during staying of the auther at the Japan Atomic Energy Research Institute (JAERI). The author takes pleasure in acknowledging valuable discussions with Drs. Azumi, Takizuka, Tani, and other members of JAERI. Director Yoshikawa of JAERI and Professor Okuda of Nagoya University are sincerely acknowledged for their encouragement to carry out this study. The author wishes to thank Dr. Takamura and Mr. Yamada of Nagoya University for detailed discussions.

The numerical computations were carried out with the FACOM M-380 computers of JAERI Computer Center.

Appendix

Taylor expanding the term in the bracket of RHS of Eq. (48a) for $\sqrt{\alpha}\tau_j \ll 1$, we write RHS of Eq. (30a) approximately as

$$\Delta v^{TP}_{\pm,j+1} = \mp 2\beta_j \alpha \tau_j sn\sqrt{\alpha}\, t_j dn\sqrt{\alpha}\, t_j. \tag{A.1}$$

With Eq. (29) and the rough replacement of $dn\sqrt{\alpha}\, t_j \sim 1/2$, the above equation is rewritten as

$$\Delta v^{TP}_{\pm,j+1} \fallingdotseq \mp \alpha\tau_0 \sin\left(\frac{\varphi_j}{2}\right) + \frac{\alpha}{v_0} O\left(\frac{v_j - v_0}{v_0}\right). \tag{A.2}$$

In deriving this equation, τ_j is also linearlized as

$$\tau_j \fallingdotseq \tau_0 \left(2 - \frac{v_j}{v_0}\right). \tag{A.3}$$

The second term of RHS of Eq. (A.2) is small compared to the first term, which will be ascertained later.

Similarly, Eq. (48b) is approximated as

$$\Delta v^{UT}_{\pm,j+1} = \mp 2\sigma\alpha\tau_j sn\beta_j\sqrt{\alpha}\, t_j cn\beta_j\sqrt{\alpha}\, t_j. \tag{A.4}$$

With Eq. (32) and the rough replacement of $cn\beta_j\sqrt{\alpha}\, t_j \sim 1/2$, the above equation is rewritten as

$$\Delta v^{UT}_{\pm,j+1} \fallingdotseq \mp \alpha\tau_0 \sin\left(\frac{\varphi_j}{2}\right) + \frac{\alpha}{v_0} O\left(\frac{v_j - v_0}{v_0}\right). \tag{A.5}$$

Eq. (A.5) coincides with Eq. (A.2) in the first order of the approximation. This means that there may be no marked difference in the dynamics between the trapped particles and the untrapped ones when the wave amplitude is small ($\sqrt{\alpha}\tau \ll 1$).

Next we linearlize RHS of Eq. (52) as

$$\Delta\varphi_{j+1} = k\left[2\pi R\left(1-\frac{2}{v_0}\right)+\frac{2\pi R}{v_0}\frac{v_{j+1}}{v_0}\right] + \frac{kl}{v_0}O\left(\frac{v_{j+1}-v_j}{v_0}\right). \tag{A.6}$$

The second term of RHS of Eq. (A.6) is small compared to the first term, which will also be ascertained later. From Eqs. (A.2), (A.5), and (A.6), the mapping equations (47) are approximated as

$$v_{j+1} - v_j = -\alpha\tau_0 \sin\left(\frac{\varphi_j}{2}\right), \tag{A.7a}$$

$$\varphi_{j+1} - \varphi_j = 2\pi kR\left(\frac{v_{j+1}}{v_0^2}-\frac{2}{v_0}+1\right). \tag{A.7b}$$

Introducing the new variables,

$$\tilde{v}_j = \frac{\pi kR}{v_0^2}\left[v_j+v_0(v_0-2)\right] \tag{A.8}$$

and

$$\tilde{\varphi}_j = \frac{\varphi_j}{2}, \tag{A.9}$$

we can reduce Eqs. (A.7) to

$$\tilde{v}_{j+1} - \tilde{v}_j = A\sin\tilde{\varphi}_j, \tag{A.10a}$$

$$\tilde{\varphi}_{j+1} - \tilde{\varphi}_j = \tilde{v}_{j+1}, \tag{A.10b}$$

where $A = (\pi R/lv_0)\alpha\tau_0^2$. This is a well-known form of the standard mapping.[22]

Let us estimate the order of the second terms of RHS's of Eqs. (A.2) and (A.6). Since $|\tilde{v}_{j+1}-\tilde{v}_j| \sim A$ from Eq. (A.9), we get

$$|v_{j+1}-v_j| \sim \frac{A}{200\pi} \tag{A.11}$$

in the present case. Then the second term of RHS of Eq. (A.2) is

estimated to be

$$\frac{\alpha}{v_0} O\left(\frac{v_j - v_0}{v_0}\right) \sim \frac{\alpha A}{200\pi} \ll \alpha\tau_0, \tag{A.12}$$

and that of Eq. (A.6) is estimated to be

$$\frac{k\,l}{v_0} O\left(\frac{v_{j+1} - v_j}{v_0}\right) \sim \frac{k\,l A}{200\pi} \ll kR. \tag{A.13}$$

References

1) A.A. Vedenov, E.P. Velikhov, and R.Z. Sagdeev: Nucl. Fusion, Suppl. Pt.2 (1962) 465.

2) W.E. Drummond and D. Pines: Nucl. Fusion, Suppl. Pt.3 (1962) 1049.

3) A.A. Vedenov: Plasma Phys. 5 (1963) 169.

4) C.F. Kennel and F. Engelmann: Phys. Fluids 9 (1966) 2377.

5) R. Klima and V.L. Sizonenko: Plasma Phys. 17 (1975) 463.

6) A.A. Galeev and R.S. Sagdeev: Reviews of Plasma Physics, Vol. 7, pp. 1, Consultants Bureau (1979).

7) R.W. Flynn: Phys. Fluids 14 (1971) 956.

8) K.N. Graham and J.A. Fejer: Phys. Fluids 19 (1976) 1054.

9) F. Doveil and D. Gresillon: Phys. Fluids 25 (1982) 1396.

10) G. Lavail and D. Pesme: Phys. Fluids 26 (1983) 52.

11) T.H. Dupree: Phys. Fluids 9 (1966) 1773.

12) J. Weinstock: Phys. Fluids 12 (1969) 1045.

13) O. Ishihara and A. Hirose: Phys. Fluids 28 (1985) 2159.

14) T. O'Neil: Phys. Fluids 8 (1965) 2255.

15) V.E. Zakharov and V.I. Karpman: Sov. Phys. JETP 16 (1963) 351.

16) R. Sugihara, Y. Midzuno, and M. Fukuda: J. Phys. Soc. Jpn. 50 (1981) 2442.

17) N.J. Fisch: Phys. Rev. Lett. 41 (1978) 873.

18) For examples, PLT; F. Jobes, J. Stevens, *et al.*: Phys. Rev. Lett. 52 (1984) 1005, Alcator-C; M. Porkolab, J.J. Schuss, *et al.*: Phys. Rev. Lett. 53 (1984) 450, JIPP T-2; K. Ohkubo, S. Takamura, *et al.*: Nucl. Fusion 22 (1982) 203.

19) S.E. Bodner: J. Plasma Phys. 5 (1971) 141.

20) G.R. Smith and B.I. Cohen: Phys. Fluids 26 (1983) 238.

21) B. Hafizi and R.E. Aamodt: Phys. Fluids 26 (1983) 1846.

22) B.V. Chirikov: Phys. Rep. 52 (1979) 263.

Table I.

α	2.5×10^{-3}	1.0×10^{-2}
$\sqrt{\alpha}\tau$	1.0	2.0
$\lvert F\rvert_{max}$	3.3×10^{-6}	4.6×10^{-5}
$\lvert D\rvert_{max}$	4.5×10^{-7}	5.7×10^{-6}
$\lvert \partial D/\partial v\rvert_{max}$	3.5×10^{-6}	7.3×10^{-5}
$\lvert F-\partial D/\partial v\rvert_{max}$	5.6×10^{-7}	4.4×10^{-5}

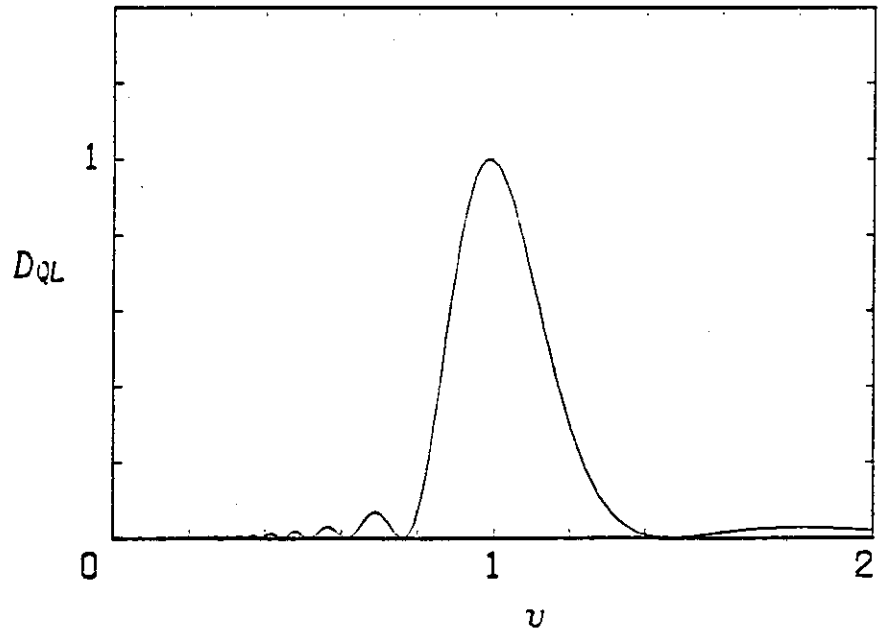

Fig. 1 Quasilinear diffusion coefficient which is given by Eq. (16).

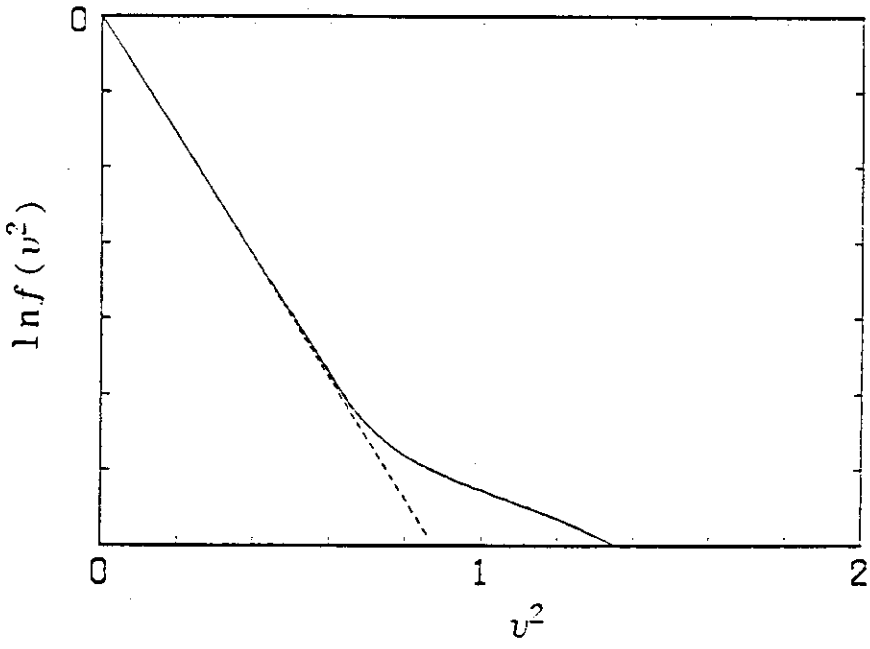

Fig. 2 Quasi-steady state distribution function obtained from the quasilinear theory Eq.(23); $\alpha = 2.5 \times 10^{-3}$ and $vt = 0.25$. The dashed line is that in the negative v.

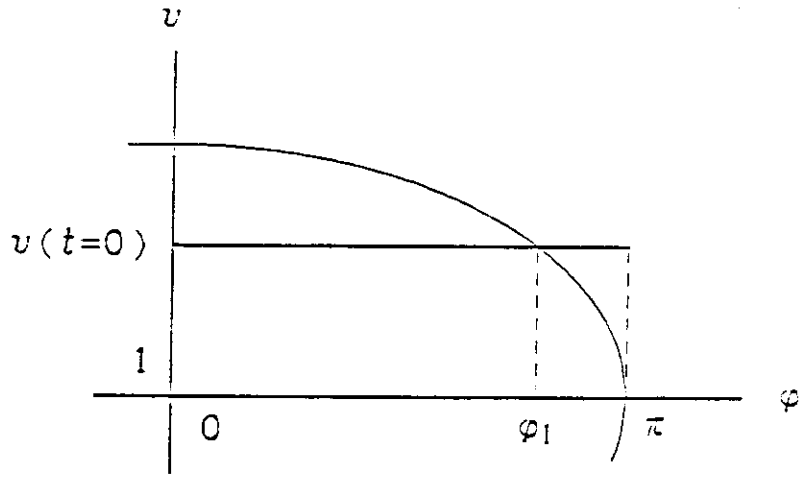

Fig. 3 Integration contour in Eqs. (41) and (42), in which $0 < \varphi < \varphi_1$ is the trapped particle part and $\varphi_1 < \varphi < \pi$ is the untrapped part.

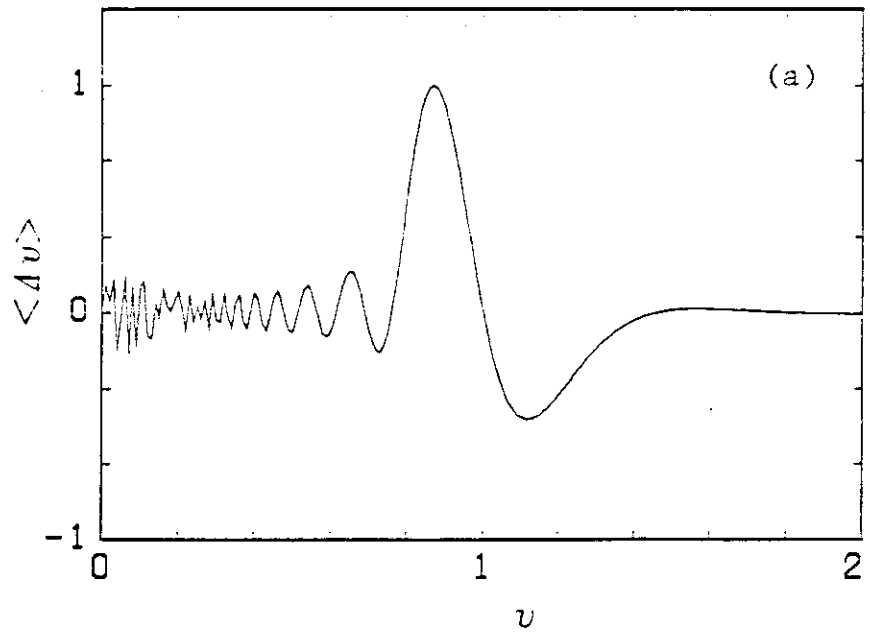

Fig. 4 (a) Mean deviation of the particle velocity for $\alpha = 2.5 \times 10^{-3}$.

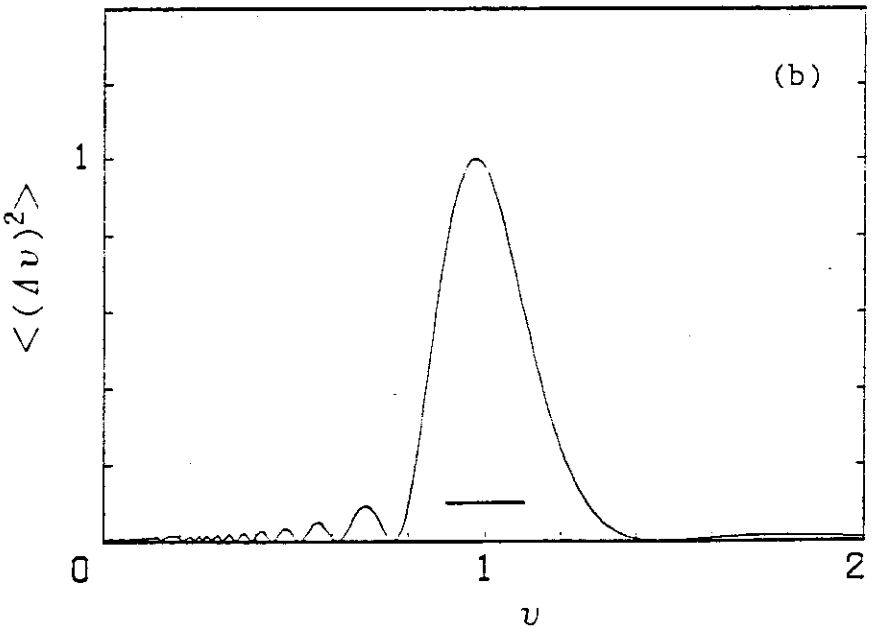

(b) Mean square deviation of the particle velocity for $\alpha = 2.5 \times 10^{-3}$. The bar indicates the trapping region, $1-2\sqrt{\alpha} \leq v \leq 1+2\sqrt{\alpha}$, where $2\sqrt{\alpha}$ is the trapping velocity.

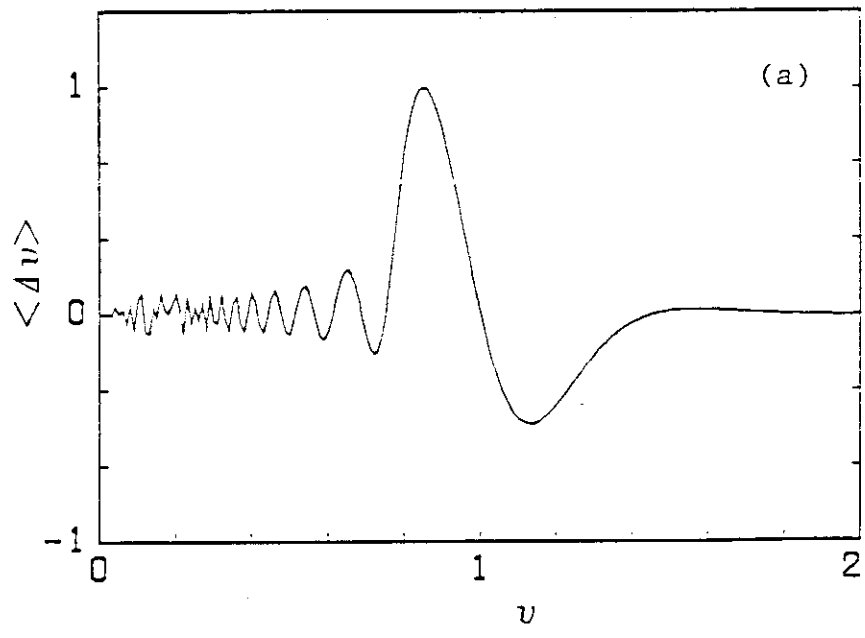

Fig. 5 (a) Mean deviation of the particle velocity for $\alpha = 1.0 \times 10^{-2}$.

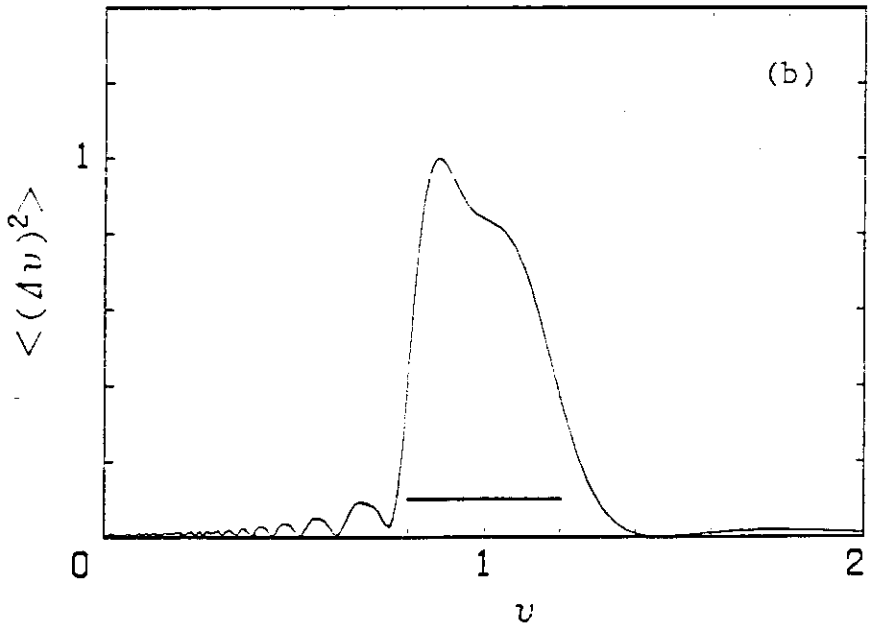

(b) Mean square deviation of the particle velocity for $\alpha = 1.0 \times 10^{-2}$. The bar indicates the trapping region, $1-2\sqrt{\alpha} \leq v \leq 1+2\sqrt{\alpha}$.

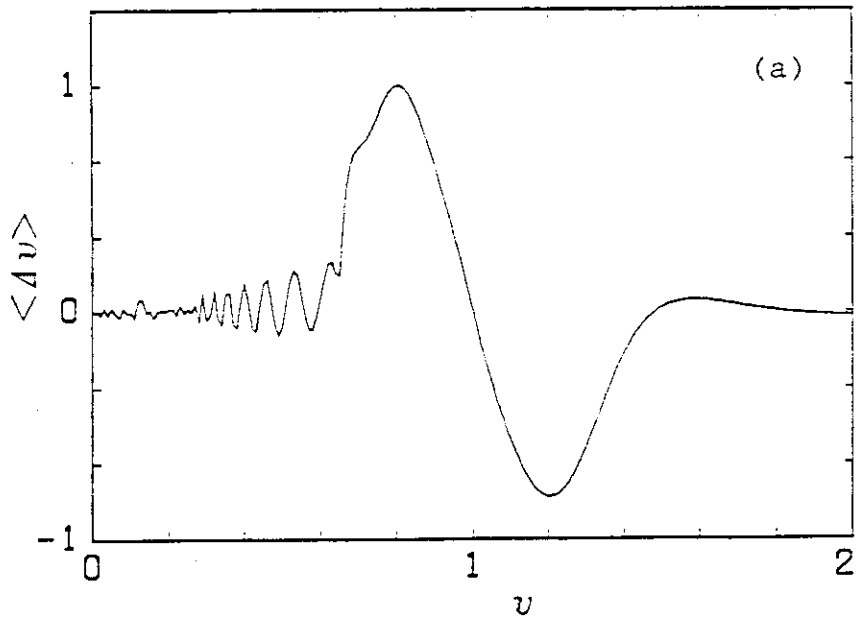

Fig. 6 (a) Mean deviation of the particle velocity for $\alpha = 3.0 \times 10^{-2}$.

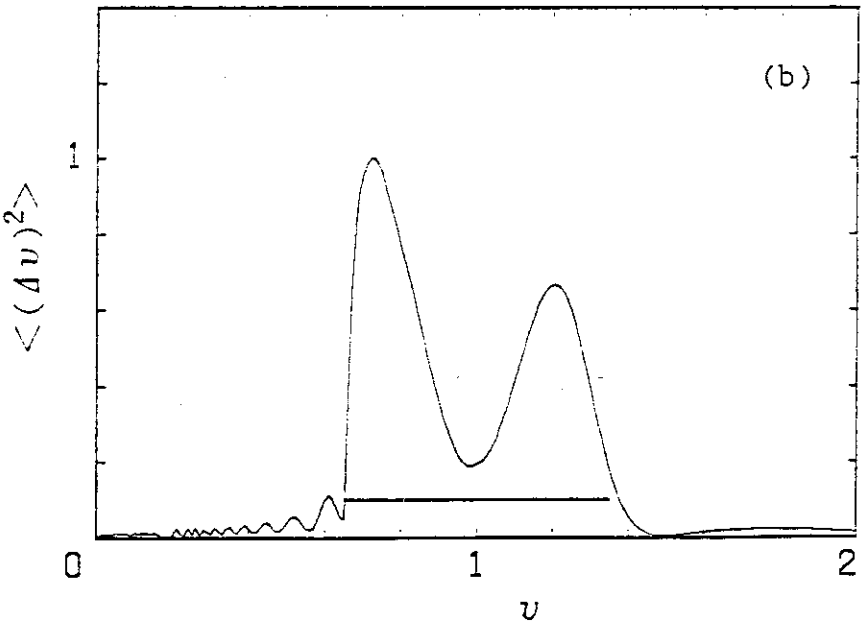

(b) Mean square deviation of the particle velocity for $\alpha = 3.0 \times 10^{-2}$. The bar indicates the trapping region, $1-2\sqrt{\alpha} \leq v \leq 1+2\sqrt{\alpha}$.

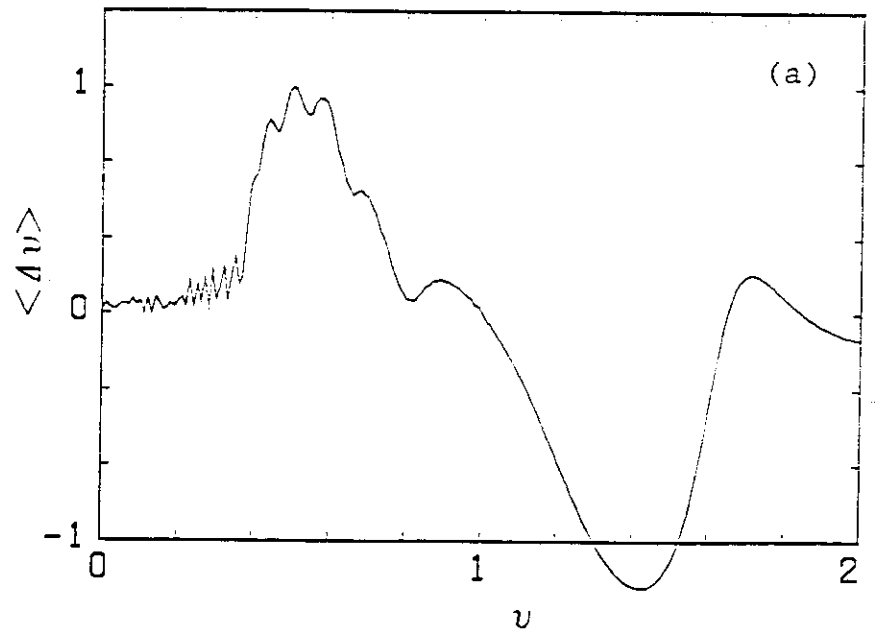

Fig. 7 (a) Mean deviation of the particle velocity for $\alpha = 0.1$.

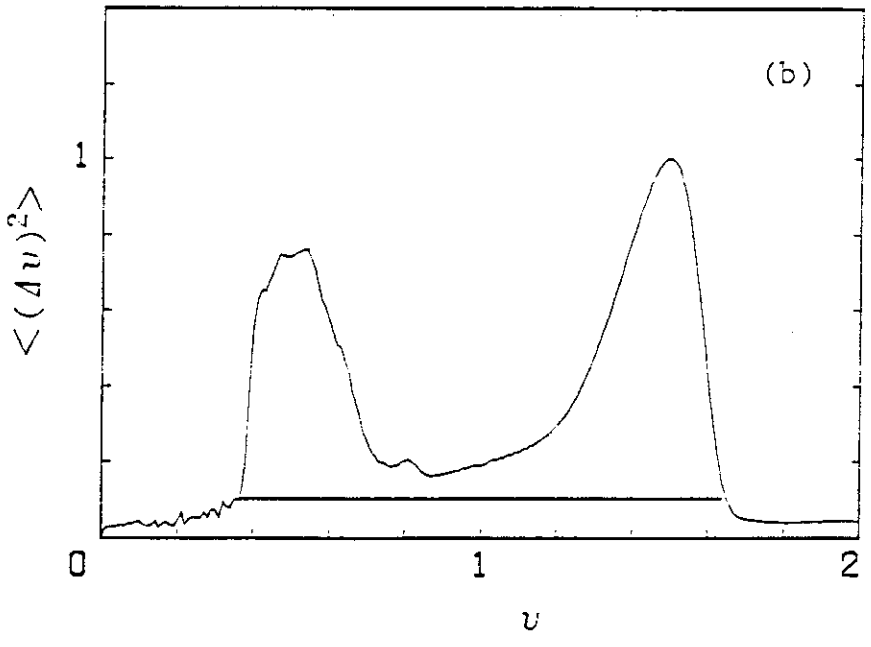

(b) Mean square deviation of the particle velocity for $\alpha = 0.1$. The bar indicates the trapping region, $1-2\sqrt{\alpha} \leq v \leq 1+2\sqrt{\alpha}$.

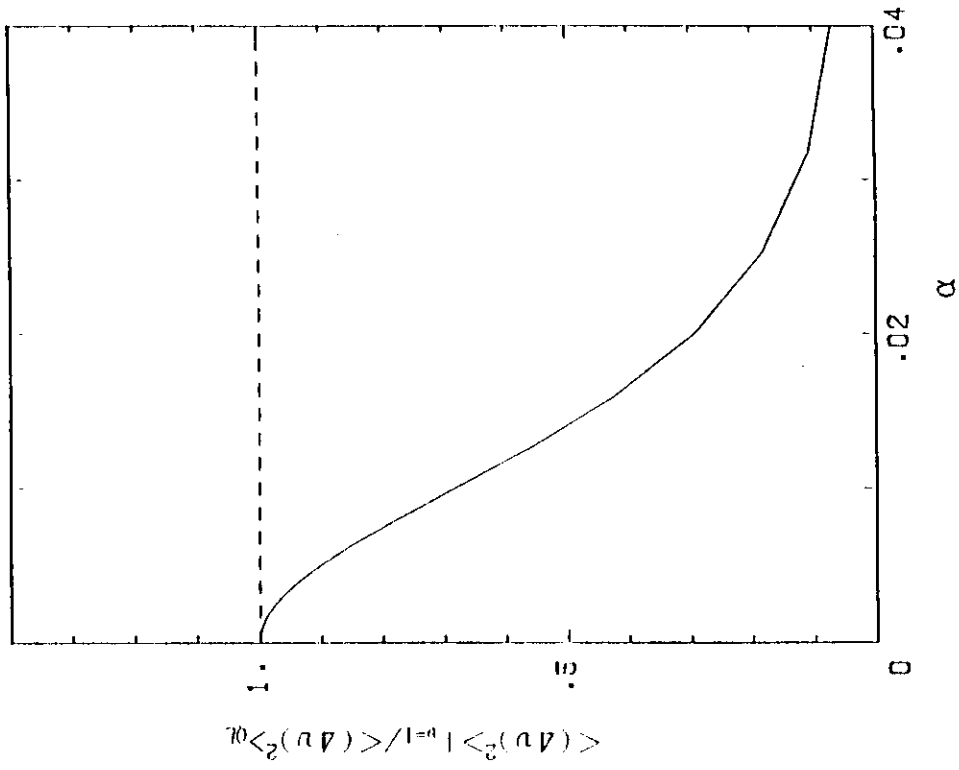

Fig. 9 Mean square deviation of the resonance particle velocity normalized to that obtained from the quasilinear theory as a function of α.

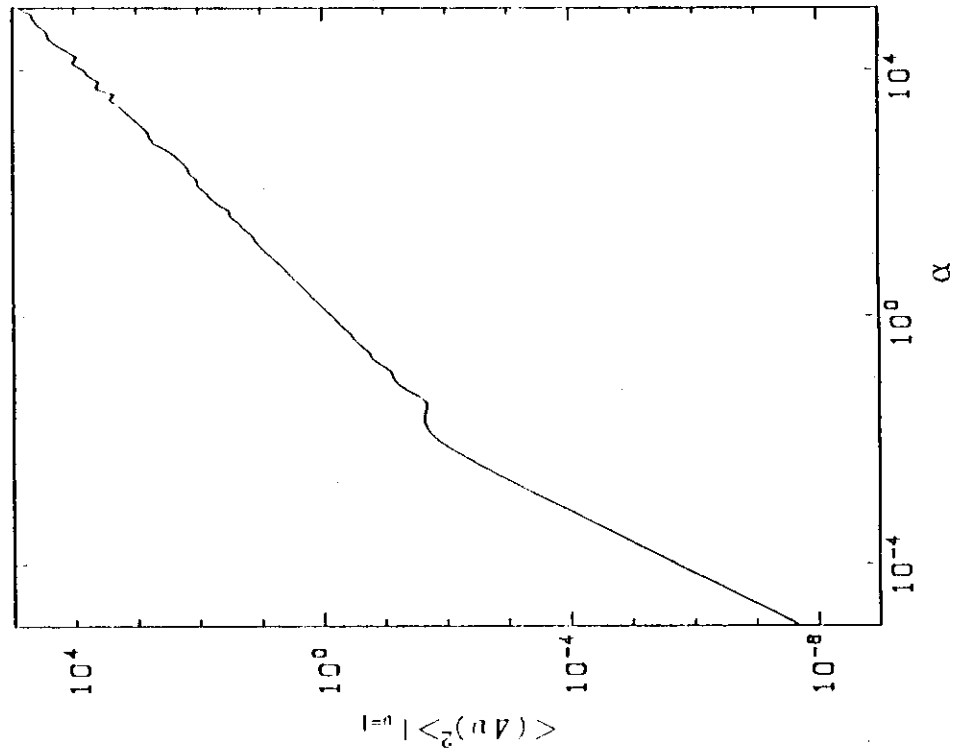

Fig. 8 Mean square deviation of the resonance particle velocity as a function of the normalized wave amplitude.

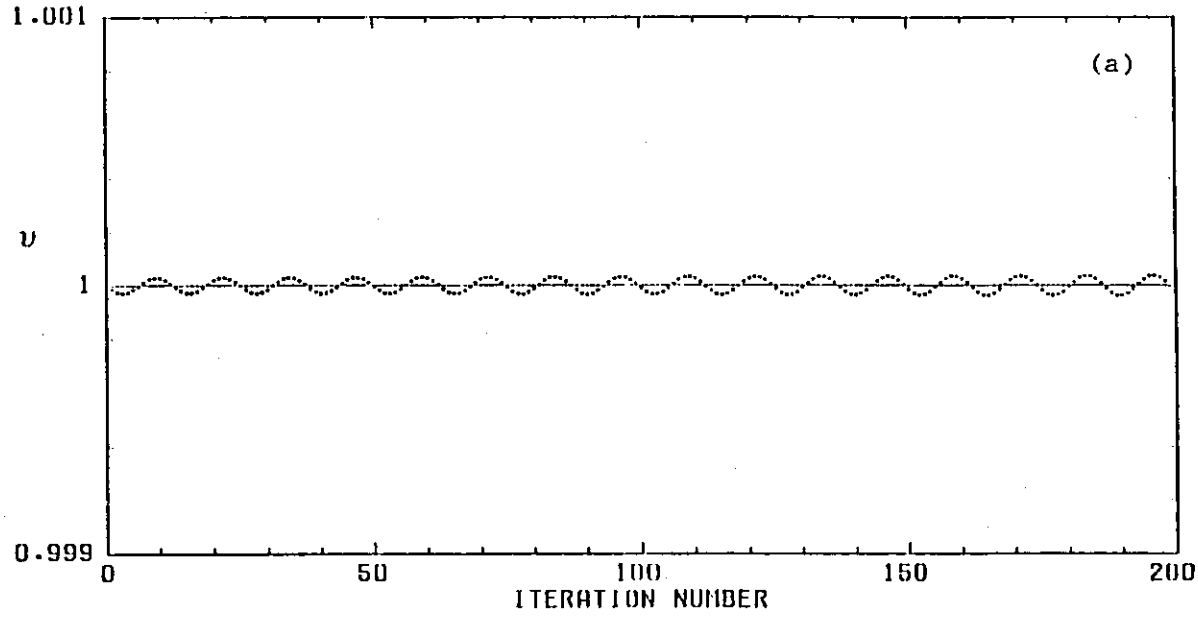

Fig. 10 Temporal changes of the particle velocity which are obtained from the mapping equations (48).
(a) $\alpha = 5.0 \times 10^{-6}$, $(u_0, \varphi_0) = (1.0, 3.0)$.

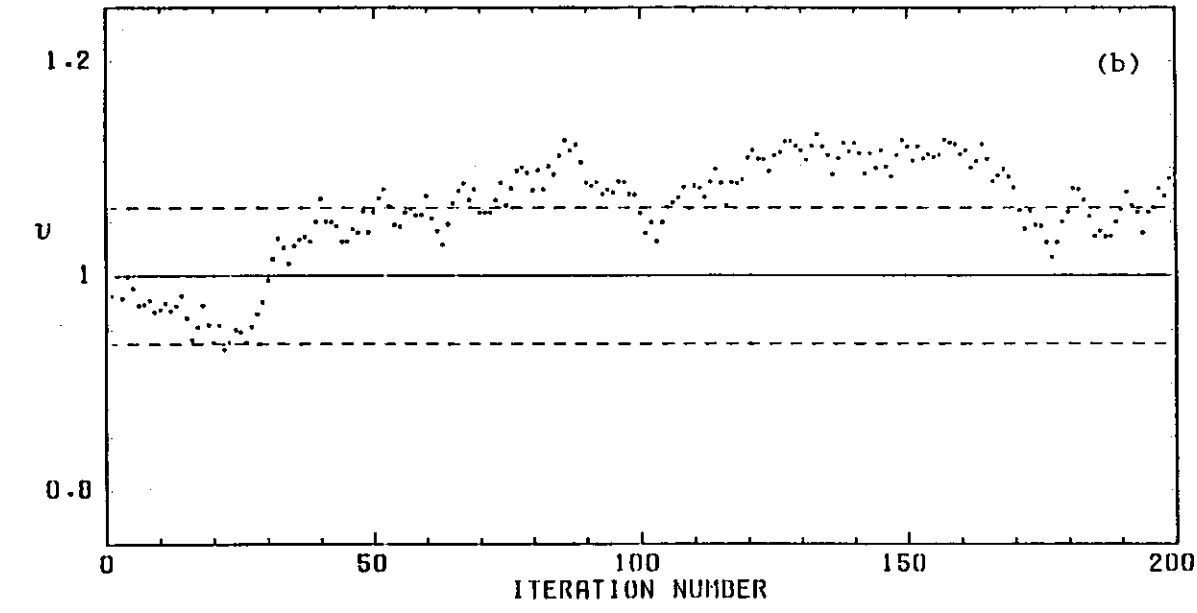

(b) $\alpha = 1.0 \times 10^{-3}$, $(u_0, \varphi_0) = (1.0, 2.0)$.

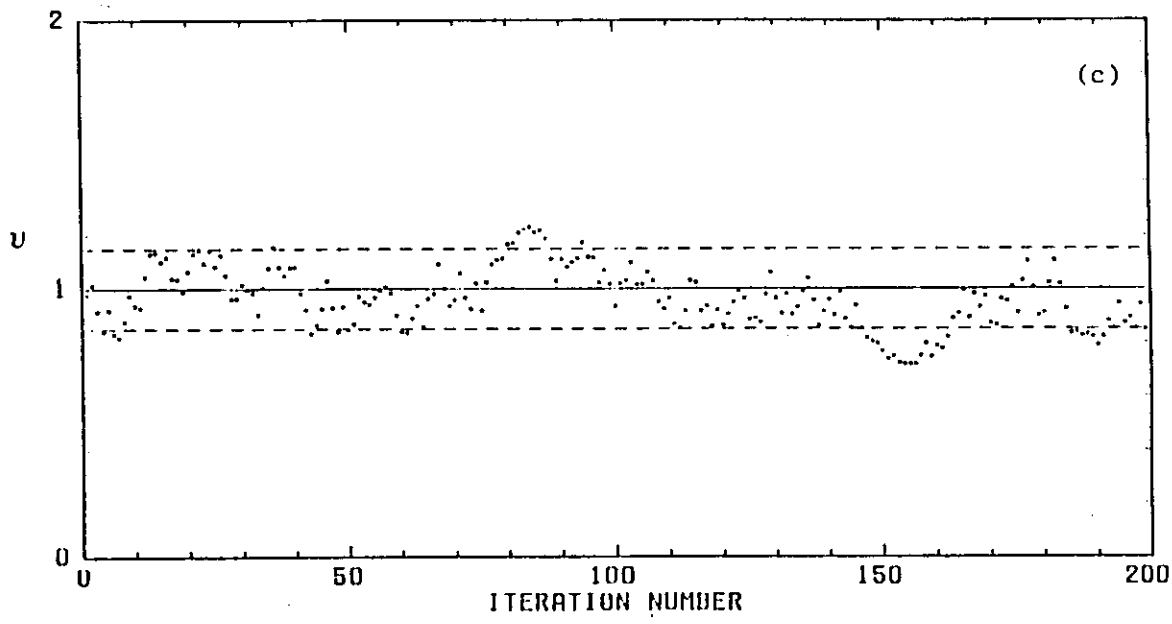

(c) $\alpha = 5.625 \times 10^{-3}$, $(u_0, \varphi_0) = (1.0, 3.0)$.

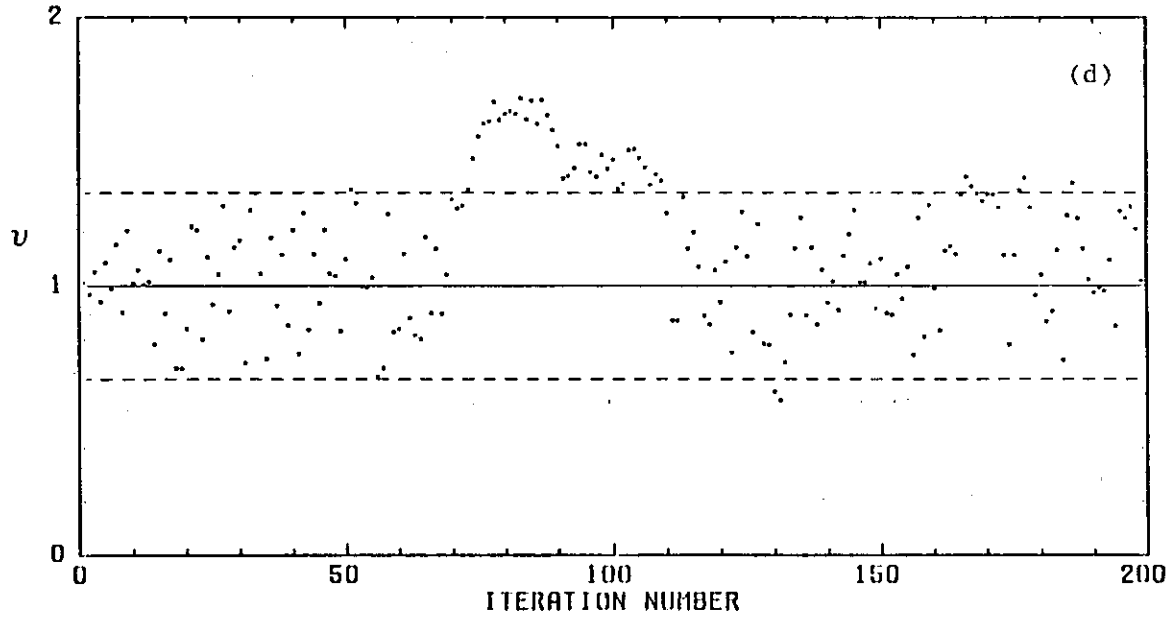

(d) $\alpha = 3.0 \times 10^{-2}$, $(u_0, \varphi_0) = (1.0, 0.25)$.

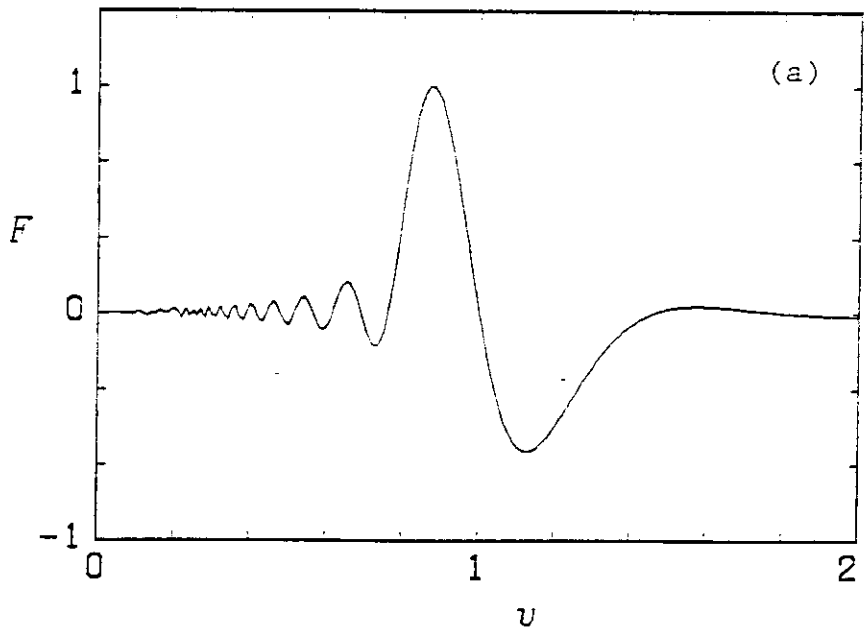

Fig. 11 (a) Friction coefficient which is given by Eqs. (15) and (41) for $\alpha = 2.5 \times 10^{-3}$ or $\sqrt{\alpha}\tau = 1.0$ when $\tau = 20$.

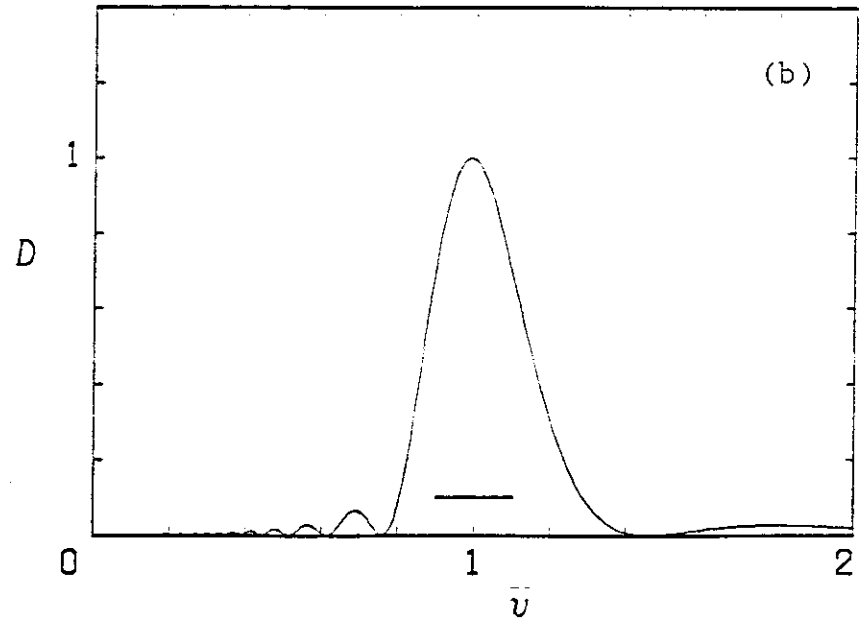

(b) Diffusion coefficient which is given by Eqs. (16) and (42) for the same value of α in (a). The bar indicates the trapping region, $1-2\sqrt{\alpha} \leq \upsilon \leq 1+2\sqrt{\alpha}$.

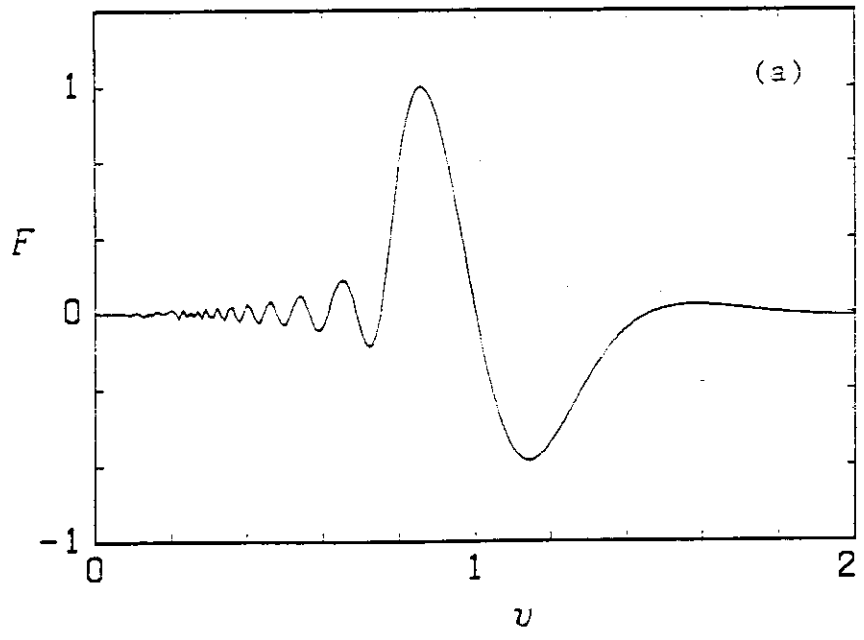

Fig. 12 (a) Friction coefficient which is given by Eqs. (15) and (41) for $\alpha = 1.0 \times 10^{-2}$ or $\sqrt{\alpha}\tau = 2.0$ when $\tau = 20$.

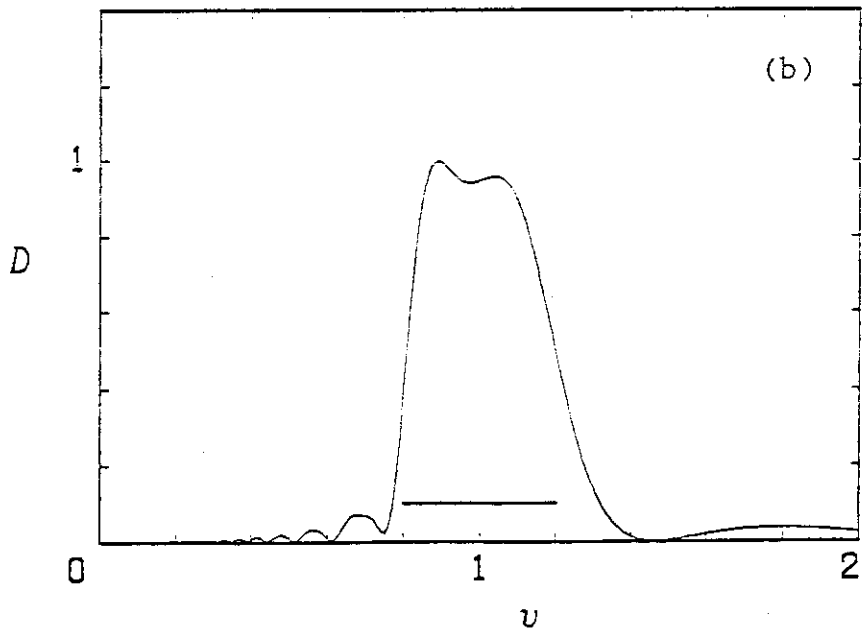

(b) Diffusion coefficient which is given by Eqs. (16) and (42) for the same value of α in (a). The bar indicates the trapping region, $1-2\sqrt{\alpha} \leq \upsilon \leq 1+2\sqrt{\alpha}$.

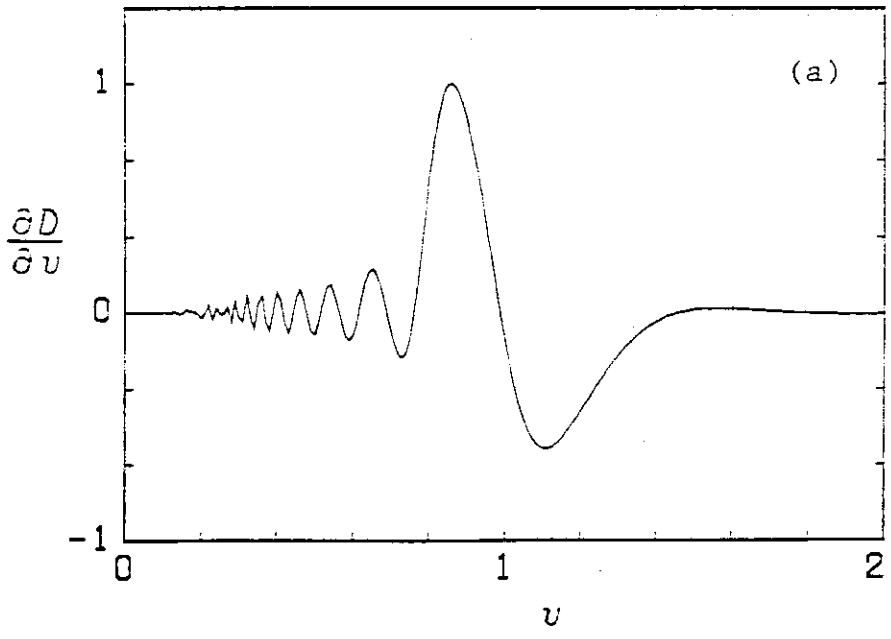

Fig. 13 (a) Diffusion coefficient differentiated by velocity, $\partial D/\partial v$, for $\alpha = 1.0 \times 10^{-2}$.

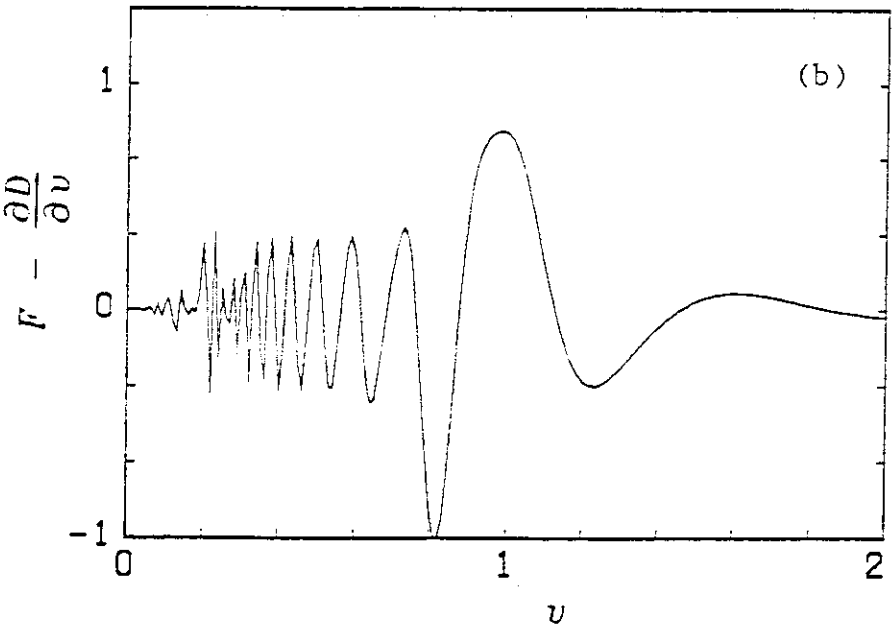

(b) Difference between the friction coefficient and the diffusion coefficient differentiated by velocity, $F-\partial D/\partial v$, for $\alpha = 1.0 \times 10^{-2}$.

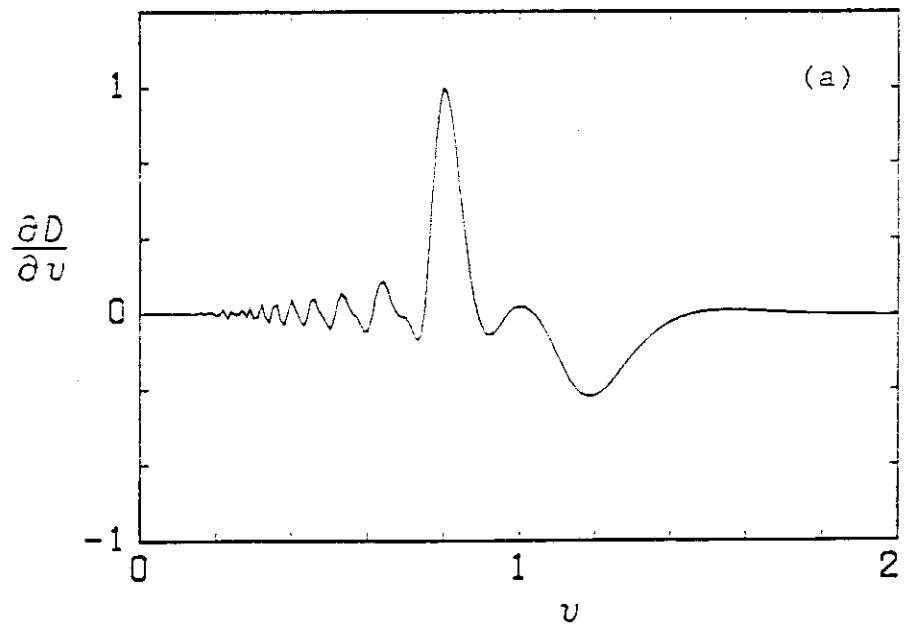

Fig. 14 (a) Diffusion coefficient differentiated by velocity, $\partial D/\partial v$, for $\alpha = 3.0 \times 10^{-2}$.

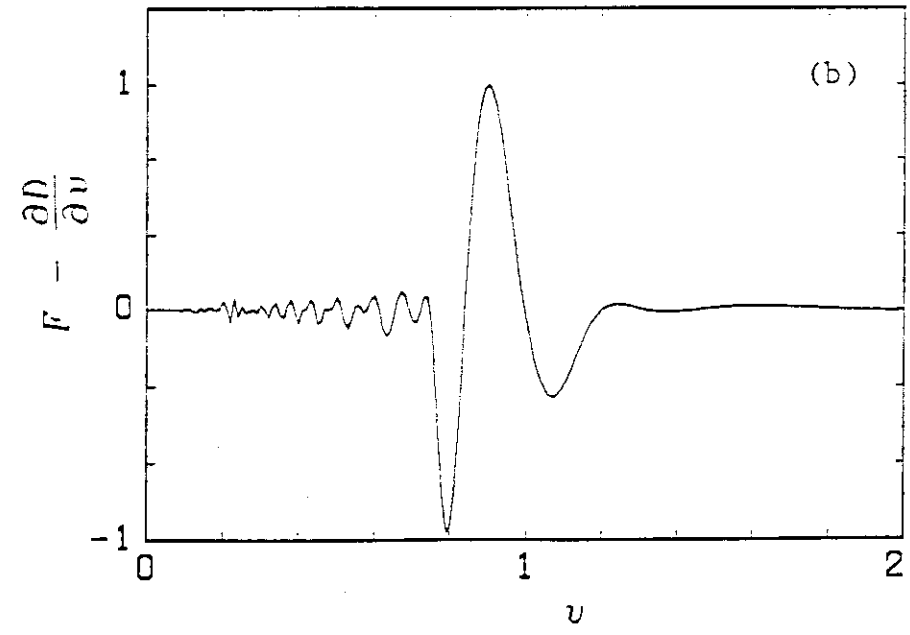

(b) Difference between the friction coefficient and the diffusion coefficient differentiated by velocity.
$F-\partial D/\partial v$, for $\alpha = 3.0 \times 10^{-2}$.

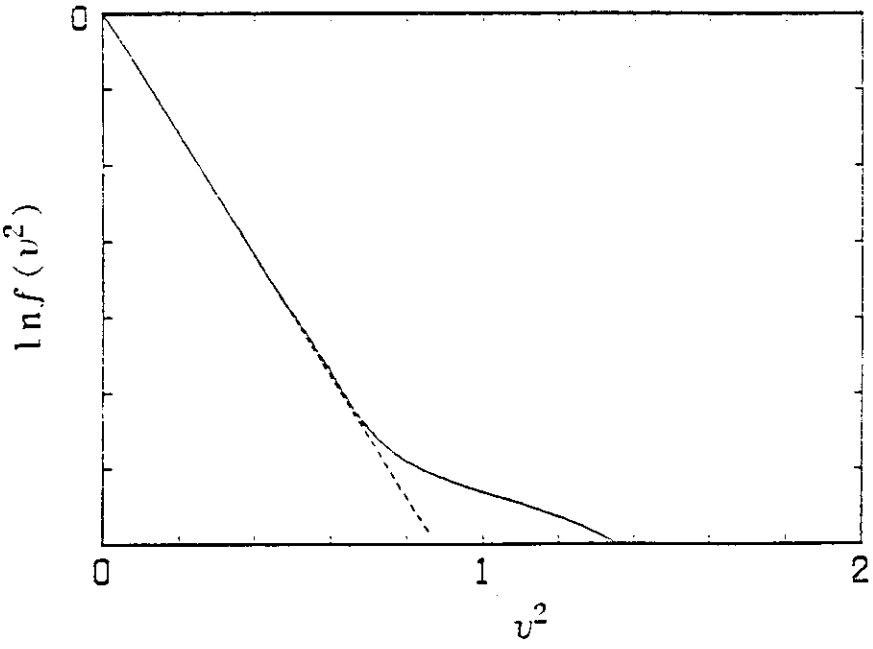

Fig. 15 Electron distribution function in a quasi-steady state which is given by Eq. (56); $\alpha = 2.5 \times 10^{-3}$ and $v_t = 0.25$. Dashed line is that in the negative part of v.

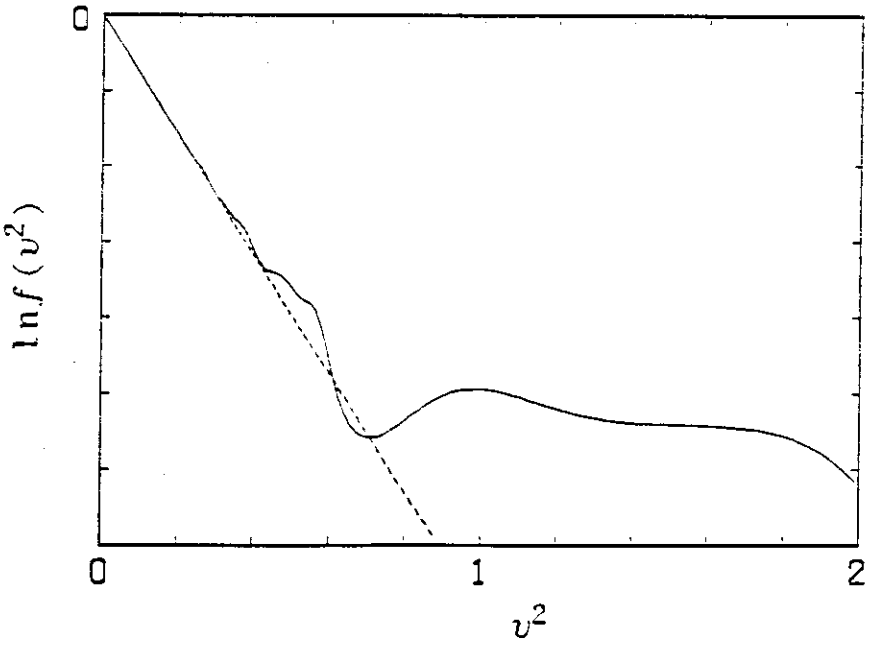

Fig. 16 Electron distribution function in a quasi-steady state which is given by Eq. (56); $\alpha = 1.0 \times 10^{-2}$ and $v_t = 0.25$. Dashed line is that in the negative part of v.

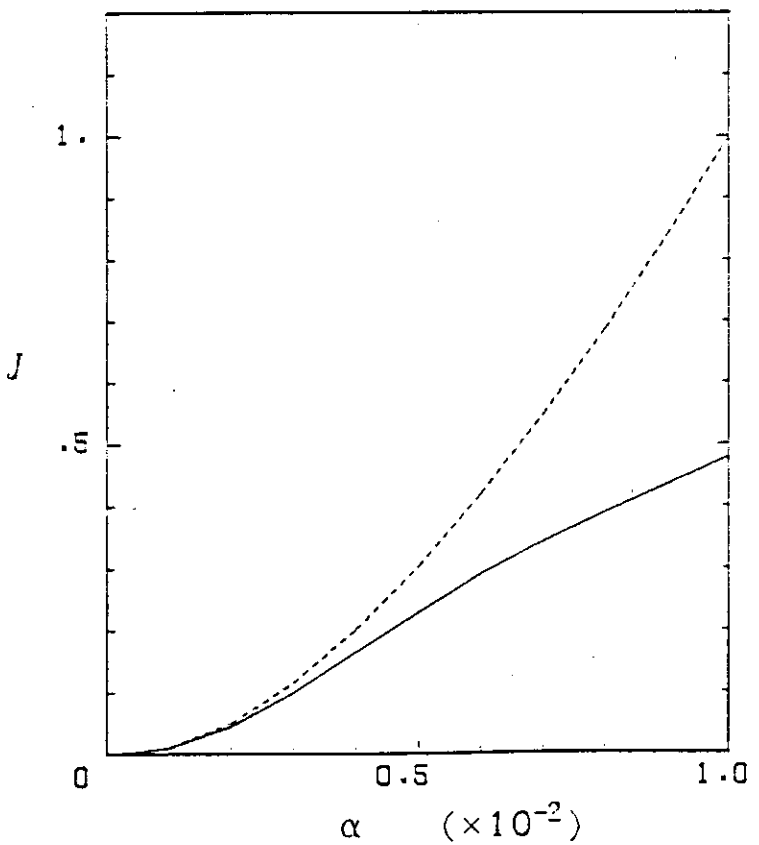

Fig. 17
Wave induced current as a function of the normalized wave amplitude; v_t = 0.25. Dashed line is that calculated from the quasilinear theory, and the solid line is that calculated from Eqs. (56) and (57).

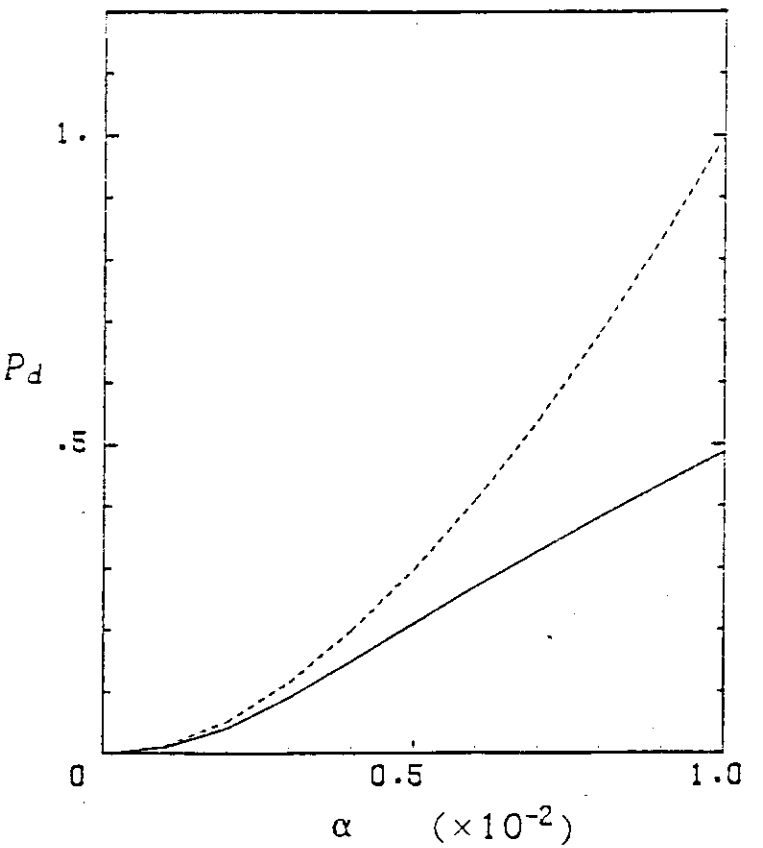

Fig. 18
Dissipated power as a function of the normalized wave amplitude; v_t = 0.25. Dashed line is that calculated from the quasilinear theory, and the solid line is that calculated from Eqs. (56) and (58).

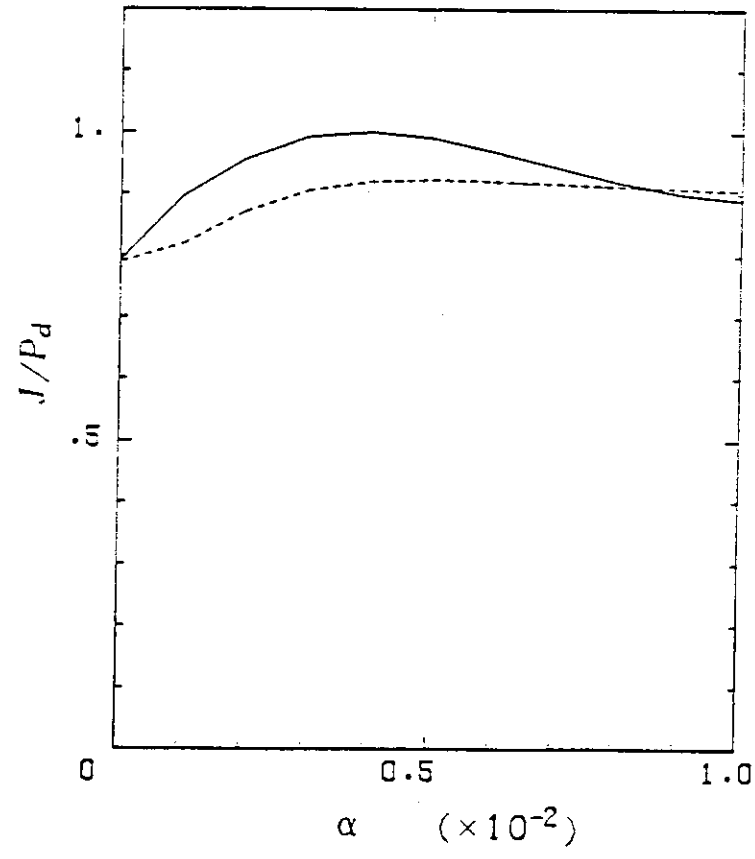

Fig. 19 Ratio of the induced current to the dissipated power as a function of the normalized wave amplitude; υ_t = 0.25. Dashed line is that calculated from the quasilinear theory, and the solid line is that calculated from Eqs. (56), (57), and (58).